


## RESEARCH ARTICLE

# Extracellular vesicles from periodontal pathogens regulate hepatic steatosis via Toll-like receptor 2 and plasminogen activator inhibitor-1

Hyun Young Kim<sup>1,4</sup> | Younggap Lim<sup>1</sup> | Ji Sun Jang<sup>2</sup> | Yeon Kyeong Ko<sup>3</sup> |  
Youngnim Choi<sup>3,4</sup> | Hong-Hee Kim<sup>2,4</sup> | Bong-Kyu Choi<sup>1</sup> 

<sup>1</sup>Department of Oral Microbiology and Immunology, School of Dentistry, Seoul National University, Seoul, Republic of Korea

<sup>2</sup>Department of Cell and Developmental Biology, School of Dentistry, Seoul National University, Seoul, Republic of Korea

<sup>3</sup>Department of Immunology and Molecular Microbiology, School of Dentistry, Seoul National University, Seoul, Republic of Korea

<sup>4</sup>Dental Research Institute, School of Dentistry, Seoul National University, Seoul, Republic of Korea

## Correspondence

Bong-Kyu Choi, Department of Oral Microbiology and Immunology, School of Dentistry, Seoul National University, 101 Daehak-ro, Jongno-gu, Seoul 03080, Republic of Korea. Email: [bongchoi@snu.ac.kr](mailto:bongchoi@snu.ac.kr)

## Funding information

National Research Foundation of Korea, Grant/Award Number: NRF-2022R1C1C2007752; Dental Research Institute of Seoul National University

## Abstract

Plasminogen activator inhibitor-1 (PAI-1) is associated with nonalcoholic fatty liver disease (NAFLD) by lipid accumulation in the liver. In this study, we showed that extracellular vesicles (EVs) from the periodontal pathogens *Filifactor alocis* and *Porphyromonas gingivalis* induced steatosis by inducing PAI-1 in the liver and serum of mice fed a low-fat diet. PAI-1 induction was not observed in TLR2<sup>-/-</sup> mice. When tested using HEK-Blue hTLR2 cells, human TLR2 reporter cells, the TLR2-activating ability of serum from NAFLD patients ( $n = 100$ ) was significantly higher than that of serum from healthy subjects ( $n = 100$ ). Correlation analysis confirmed that PAI-1 levels were positively correlated with the TLR2-activating ability of serum from NAFLD patients and healthy subjects. Amphiphilic molecules in EVs were involved in PAI-1 induction. Our data demonstrate that the TLR2/PAI-1 axis is important for hepatic steatosis by EVs of periodontal pathogens.

## KEYWORDS

extracellular vesicle, nonalcoholic fatty liver disease, periodontal pathogen, plasminogen activator inhibitor-1, Toll-like receptor 2

## 1 | INTRODUCTION

Nonalcoholic fatty liver disease (NAFLD) is the most common liver disease and is characterized by excessive hepatic lipid accumulation without heavy alcohol consumption. NAFLD represents stages between nonalcoholic fatty liver (NAFL) and non-alcoholic steatohepatitis (NASH), which is a major cause of hepatic fibrosis and cirrhosis leading to liver cancer and liver death (Chalasani et al., 2012; Ekstedt et al., 2017). NAFLD is a multifactorial disease influenced by multiple factors, including obesity, diabetes, and genetic factors (Yu et al., 2019). Recently, microbiota has gained attention as a causal factor of NAFLD progression (Aron-Wisniewsky et al., 2020) and microbiota signatures are regarded as useful diagnostic tools for NAFLD (Lee et al., 2020). The gut microbiota contributes to NAFLD progression via various mechanisms, such as alcohol production and inhibition of total bile acid synthesis (Cani et al., 2007; Sayin et al., 2013; Zhu et al., 2013). Microbe-associated molecular patterns (MAMPs) activate Toll-like receptors (TLRs), which can cause liver inflammation and NAFLD (Miura & Ohnishi, 2014). Serum from NAFLD patients contains higher concentrations of lipopolysaccharide (LPS), a representative TLR4 ligand, than that from

This is an open access article under the terms of the [Creative Commons Attribution-NonCommercial-NoDerivs License](https://creativecommons.org/licenses/by-nc-nd/4.0/), which permits use and distribution in any medium, provided the original work is properly cited, the use is non-commercial and no modifications or adaptations are made.

© 2024 The Authors. *Journal of Extracellular Vesicles* published by Wiley Periodicals, LLC on behalf of the International Society for Extracellular Vesicles.

control subjects, and long-term exposure to low-dose LPS increases NASH symptoms in a high-fat diet (HFD)-induced NAFLD mouse model (Carpino et al., 2020; Imajo et al., 2012).

Plasminogen activator inhibitor-1 (PAI-1) is a well-known regulator of the fibrinolysis system (Targher et al., 2008) and is produced by various cell types, including hepatocytes, vascular endothelial cells, and adipocytes (Alessi et al., 1997; Busso et al., 1994; Erickson et al., 1985). PAI-1 has received attention for its roles in metabolic syndrome (Alessi et al., 2003; Alessi & Juhan-Vague, 2006) and has been shown to be an independent risk factor for NAFLD progression (Alsharoh et al., 2022; Levine et al., 2021; Rivas et al., 2021). Patients with NAFLD showed elevated PAI-1 serum levels compared to healthy people. Mice with PAI-1 knockout were resistant to diet-induced hepatic steatosis and induction of lipid synthesis genes (Henkel et al., 2018). Periodontitis patients also showed elevated PAI-1 serum levels compared to healthy people (Bizzarro et al., 2007). *Porphyromonas gingivalis*, the keystone pathogen in periodontitis progression, increased PAI-1 expression in platelets and human aortic endothelial cells (Klarstrom Engstrom et al., 2015; Roth et al., 2006). Although PAI-1 induction by periodontal pathogens appears to be important for NAFLD progression, the molecular mechanisms of PAI-1 induction by periodontal pathogens in the liver have not been investigated.

The oral microbiota is the second largest microbiota after the gut microbiota and contains more than 700 species of microorganisms (Sender et al., 2016). Dysbiosis of the oral microbiota can cause periodontitis, which is one of the most common inflammatory diseases leading to tooth-supporting tissue destruction and tooth loss (Kinane et al., 2017). Periodontitis and NAFLD share risk factors, including diabetes, obesity and metabolic syndrome (Genco & Borgnakke, 2013). Epidemiological studies have determined that periodontitis is an independent risk factor for liver diseases, including NAFLD (Akinkugbe et al., 2017; Helenius-Hietala et al., 2019; Yoneda et al., 2012). In NAFLD patients, periodontal treatment decreased aspartate aminotransferase (AST) and alanine aminotransferase (ALT) levels, which are markers of liver damage (Yoneda et al., 2012). Furthermore, infection by periodontal pathogens is regarded as a risk factor for NAFLD. Gram-negative periodontal pathogens, *P. gingivalis* and *Treponema denticola*, were more frequently detected in patients with NAFLD than in non-NAFLD subjects (Sato et al., 2022; Yoneda et al., 2012). Animal studies have shown that gram-negative periodontal pathogens, including *P. gingivalis* and *Aggregatibacter actinomycetemcomitans*, aggravate liver steatosis, glucose intolerance and insulin resistance in a high-fat diet-induced NAFLD model (Komazaki et al., 2017; Yoneda et al., 2012).

Extracellular vesicles (EVs) released by bacteria are nanosized particles surrounded by a lipid bilayer (Toyofuku et al., 2019). Periodontal pathogens release EVs, which are more frequently detected in saliva samples from periodontitis patients than in those from healthy subjects (Han et al., 2021). Periodontal pathogen EVs contain MAMPs, including LPS, bacterial lipoproteins, peptidoglycan, nucleic acids, and special proteins such as gingipains of *P. gingivalis* (Veith et al., 2014). Previously, we demonstrated that EVs from a representative gram-positive periodontal pathogen, *Filifactor alocis*, contain bacterial lipoproteins, which are major MAMPs that induce systemic bone resorption via TLR2 (Kim et al., 2021; Song et al., 2020). EVs from gram-negative periodontal pathogens (*P. gingivalis* and *Tannerella forsythia*) also have immunostimulatory activities through TLR2 activation (Kim et al., 2022). Recently, a study of the link between NAFLD/NASH and bacterial extracellular vesicles was reported (Fizanne et al., 2023). Faeces EVs and blood circulating EVs from NAFLD/NASH patients contain higher amounts of LPS than those from healthy subjects, and only faeces-derived EVs from NASH patients contain lipoteichoic acid (LTA), which is one of the TLR2 ligands of gram-positive bacteria. However, there is no study on the direct role of EVs from both gram-positive and gram-negative periodontal pathogens in NAFLD progression. In this study, we identified the role of EVs from a representative gram-positive periodontal pathogen, *F. alocis*, and a gram-negative periodontal pathogen, *P. gingivalis*, in liver steatosis. Continuous exposure to low-dose periodontal pathogen EVs increased liver steatosis in low-fat diet (LFD)-fed mice. The PAI-1/TLR2 axis was involved in this phenomenon. This study presents a novel molecular mechanism to explain the correlation between periodontitis and NAFLD.

## 2 | MATERIALS AND METHODS

### 2.1 | Reagents and chemicals

Columbia broth, brain heart infusion (BHI), yeast extract, and Bacto agar were purchased from BD Biosciences (San Jose, CA, USA). Hemin, vitamin K, L-cysteine, L-arginine, and resazurin were purchased from Sigma (St. Louis, MO, USA). RPMI-1640 medium and phosphate-buffered saline (PBS) were purchased from Welgene (Daegu, South Korea). Penicillin/streptomycin (P/S), foetal bovine serum (FBS), and trypsin-EDTA were purchased from Gibco BRL (Paisley, UK). TM5441, a PAI-1 inhibitor, was purchased from R&D (Minneapolis, MN, USA). Paraformaldehyde (4%) solution was purchased from Biosesang (Gyeonggi-do, South Korea). Pam3CSK4 and ultrapure LPS were purchased from InvivoGen (San Diego, CA, USA).

## 2.2 | Bacterial extracellular vesicles

Bacterial EVs were purified as previously described (Kim et al., 2020, 2021, 2022). Briefly, bacteria were grown until 48 h post inoculation, and supernatants were harvested by centrifugation (10,000×g, 4°C). Then, the supernatants were filtered through a 0.22 μm membrane filter (Corning, New York, NY, USA) and subjected to a 100 kDa cut-off centrifugal filter (Merck, Darmstadt, Germany). The crude EVs were concentrated by ultracentrifugation (160,000×g, 4°C, 2 h) using Optima XE-100 and a Type 45 Ti rotor (Beckman Coulter, Brea, CA, USA). The EVs were purified by iodixanol-based density gradient ultracentrifugation (100,000×g, 4°C, 18 h) using an SW 40 Ti rotor (Beckman Coulter). The nanoparticle-enriched fractions were concentrated by ultracentrifugation and stored at −80°C until use.

The gingipain-deficient *P. gingivalis* strain KDPI36 (*kgp*<sup>−</sup> *rgpA*<sup>−</sup> *rgpB*<sup>−</sup>) was kindly provided by Dr. Koji Nakayama (Nagasaki University, Nagasaki, Japan) and cultured as previously described (Jung et al., 2017). For EV preparation, the *P. gingivalis* WT strain (ATCC 33277) and KDP 136 were cultured for 48 h in an anaerobic chamber.

Enzyme or inhibitor treatment of EVs was performed as previously described with minor modifications (Han et al., 2019; Hashimoto et al., 2006; Kim et al., 2021, 2022; Seo & Nahm, 2009). EVs (200 μg/200 μL PBS) were treated with lipoprotein lipase from the *Pseudomonas* species (50 μg/mL), proteinase K (50 μg/mL), platelet-activating factor acetylhydrolase (PAF-AH, 50 μg/mL), polymyxin B (50 μg/mL), DNase (2 U/200 μL), or RNase (1 U/200 μL) at 37°C for 16 h. For the control, EVs (200 μg/200 μL PBS) were incubated under the same conditions without treatment. After the incubation period, EVs were ultracentrifuged (160,000×g, 4°C, 1 h) and resuspended in 200 μL PBS for further experiments.

## 2.3 | Human serum

This study was performed in accordance with the Helsinki Declaration after approvals from the Institutional Review Board of Seoul National University School of Dentistry (IRB approval No. S-D20230008), the Institutional Review Board of Seoul National University Bundang Hospital (IRB approval No. DT-2023-009-01), and the Institutional Review Board of Ajou University Hospital (IRB approval No. AJHB-2023-14). Serum samples were obtained from healthy subjects ( $n = 100$ ) and NAFLD patients ( $n = 100$ ) from the Human Bioresource Centre of Seoul National University Bundang Hospital [serum from healthy subjects (#1 – #50)] and the Biobank of Ajou University Hospital [serum from healthy subjects (#51 – #100); serum from NAFLD patients (#1 – #100)]. Information including the age and sex of these subjects is shown in Table S1.

## 2.4 | Animal

All animal experiments were approved by the Institutional Animal Care and Use Committee of Seoul National University (SNU-220628-2) and conducted in accordance with the guidelines and regulations of the institute. The animal experiments were conducted in accordance with the ARRIVE guidelines (<https://arriveguidelines.org>). C57BL/6 mice were purchased from Orient Bio (Gyeonggi-do, South Korea), and TLR2<sup>−/−</sup> mice (C57BL/6) were obtained from The Jackson Laboratory (Bar Harbor, ME, USA). Low-fat diet (LFD) chow (TD.06416, 20.1% protein, 69.8% carbohydrate, and 10.2% fat) and high-fat diet (HFD) chow (TD.06414, 18.4% protein, 21.3% carbohydrate, and 60.3% fat) were purchased from DooYeol Biotech (Seoul, South Korea).

## 2.5 | Detection of *F. alocis* proteins in mouse livers

Anti-*F. alocis* rabbit serum was obtained from AbClon Inc. (Seoul, South Korea). Briefly, 4-week-old New Zealand white rabbits were intraperitoneally immunized with heat-inactivated *F. alocis* (20 μg) containing complete Freund's adjuvant (Sigma). After 4 weeks, the rabbits were boosted with heat-inactivated *F. alocis* (20 μg) containing incomplete Freund's adjuvant (Sigma) every 2 weeks, and serum was collected 6 weeks later.

Eight-week-old C57BL/6 mice were administered Fa EVs (50 μg) by intraperitoneal injection. At 1, 3, 6, 12, and 24 h postinjection, the liver was extracted and homogenized with RIPA buffer (10 mM Tris-HCl, pH 7.5, 150 mM NaCl, 1% Triton X-100) containing complete protease inhibitor (Roche, Mannheim, Germany). Protein concentrations of liver lysates were determined by bicinchoninic acid (BCA) assays (Thermo Fisher Scientific Inc. Waltham, MA, USA). *F. alocis* components in liver lysates were detected by direct enzyme-linked immunosorbent assay (ELISA). The standard curve was prepared by serial dilution of *F. alocis* EVs (2000, 1000, 500, 250, 125, 62.5, 31.2, 15.6, 7.8 ng/mL). *F. alocis* EVs and liver lysates (2 μg/mL) were coated in EIA/RIA 96-well plates (Corning, New York, NY, USA) at 4°C for 16 h. The concentrations of *F. alocis* components in the samples were measured using anti-*F. alocis* rabbit serum (1:1000) and rabbit IgG HRP-conjugated antibody (R&D systems, 1:20000).

## 2.6 | Detection of periodontal pathogen proteins in human serum

*F. alocis* and *P. gingivalis* proteins in human serum samples were detected by direct enzyme-linked immunosorbent assay (ELISA). The standard curves were prepared by serial dilution of *F. alocis* lysates (2000, 1000, 500, 250, 125, 62.5, 31.2, 15.6, 7.8 ng/mL) and *P. gingivalis* lysates (3750, 1875, 937.5, 468.8, 234.4, 117.2, 58.6, 29.3 ng/mL). Human serum samples were diluted with PBS and coated in EIA/RIA 96-well plates (Corning, New York, NY, USA) at 4°C for 16 h. For measuring concentration of *F. alocis* and *P. gingivalis* proteins in the serum samples, each sample were incubated with anti-*F. alocis* rabbit serum (1:1000) and mouse anti-*P. gingivalis* IgG2a monoclonal antibody (1:100) (Creative Diagnostics, Shirley, NY, USA) at 25°C for 2 h, respectively. The concentrations of *F. alocis* and *P. gingivalis* proteins in the serum were detected by colorimetric method using anti-rabbit IgG HRP-conjugated antibody (R&D systems, 1:20000) and anti-mouse IgG2a HRP-conjugated antibody (Southern Biotech, Birmingham, AL, USA, 1:5000), respectively.

## 2.7 | qPCR array

Eight-week-old C57BL/6 mice were administered Fa EVs (50 µg) by intraperitoneal injection. One hour postinjection, liver mRNA was extracted using an AccuPrep Universal RNA Extraction Kit (Bioneer, Daejeon, South Korea), and the purity and quality of mRNA were measured by a NanoDrop One (Thermo Fisher Scientific Inc.) and 5200 Fragment Analyser (Agilent Technologies, Inc. Santa Clara, CA, USA) according to the Minimum Information for Publication of Quantitative Real-Time PCR Experiments (MIQE) guidelines. Complementary DNA was synthesized using AccuPower Rocketscript Cycle RT Premix (Bioneer). qPCR array was performed as previously described (Ahn et al., 2016; Hong et al., 2021). Data analysis was based on the  $2^{-\Delta\Delta C_t}$  method. Average threshold cycles ( $C_t$ ) for the gene of interest were obtained from triplicate samples and normalized by the  $C_t$  of HPRT as a housekeeping gene. The gene information is listed in Table S2.

## 2.8 | Adipokine array

Eight-week-old C57BL/6 mice were administered Fa EVs (50 µg) by intraperitoneal injection. Three hours postinjection, 100 mg of liver was homogenized with RIPA buffer containing complete protease inhibitor (Roche). Liver lysates (500 µg) were subjected to an adipokine array (R&D) to measure 38 obesity-related molecules.

## 2.9 | NAFLD experiment

NAFLD experiments were performed as previously described (Imajo et al., 2012), and experimental schemes are outlined in Figures 2a, 3a and 4a. Eight-week-old C57BL/6 mice were fed a ND or HFD for 4 weeks. Then, mice were administered Fa EVs (5 µg) or Pg EVs (5 µg) intraperitoneally twice a week for 8 weeks. For PAI-1 inhibition, mice were administered DMSO (vehicle control) or TM5441 (20 mg/kg) intraperitoneally twice a week for 8 weeks. Mice were sacrificed 1 h after the final Fa EV or Pg EV injection and used for further experiments. Body weight and food intake were measured once a week during the experimental period. Subcutaneous fat and visceral fat were excised after mouse sacrifice and weighed using a microbalance. Triglyceride concentrations in the liver and serum were measured using a triglyceride assay kit (Abcam, Cambridge, United Kingdom). Insulin, alanine aminotransferase (ALT), and aspartate aminotransferase (AST) concentrations were measured using ELISA kits (Abcam). PAI-1 concentration was measured using a PAI-1 ELISA kit (R&D). The active PAI-1 concentration was measured using an active PAI-1 DuoSet ELISA kit (Innovative Research, Novi, MI, USA). Serum glucose levels were measured using a glucose assay kit (Abcam).

## 2.10 | Liver histology

The left lateral lobe of the mouse liver was fixed in 4% paraformaldehyde at 4°C for 24 h and transferred to 30% sucrose in PBS at 4°C for 3 days. For lipid and haematoxylin staining, the liver lobe was cryosectioned on slide glass at 10 µm using a cryocut microtome 1950 (Leica, Wetzlar, Germany). For histological analysis, cryosections of the liver lobe were stained with Oil Red O and haematoxylin using an Oil Red O stain kit (Abcam) according to the manufacturer's instructions. Fibers in cryosections were stained with trichrome stain kit (Abcam) according to the manufacturer's instructions. The images were captured by bright field microscopy (Leica), and the steatosis score, liver inflammation score, and fibrosis stage were measured according to previously described criteria (Imajo et al., 2012).

## 2.11 | Cell culture and stimulation

Huh7 (Korean Cell Line Bank, KCLB No. 60104) cells, Hep3B (KCLB No. 88064) cells, HepG2 (KCLB No. 88065), SNU-449 (KCLB No. 00449), and Hepa-1c1c7 (KCLB No. 22026) cells were cultured in RPMI-1640 medium supplemented with FBS (10%) and antibiotics (100 U/mL penicillin and 100  $\mu$ g/mL streptomycin) at 37°C in a humidified incubator (5% CO<sub>2</sub>).

For ELISA and cell death assays, the cells ( $2 \times 10^5$  cells/well in 48-well plates) were incubated for 16 h in serum-free RPMI-1640 medium. Then, the cells were stimulated with bacterial EVs for the indicated time periods in serum-free RPMI-1640 medium and used for further experiments. For the PAI-1 ELISA, a PAI-1 DuoSet ELISA kit (R&D) was used according to the manufacturer's instructions. For the cell death assay, a Cell Counting Kit-8 (CCK-8, DOJINDO Laboratories, Kumamoto, Japan) assay kit was used according to the manufacturer's instructions.

For Western blotting and real-time PCR (RT-PCR) analysis, the cells ( $5 \times 10^5$  cells/well in 6-well plates) were incubated for 16 h in serum-free RPMI-1640 medium. Then, the cells were stimulated with bacterial EVs for the indicated time periods in serum-free RPMI-1640 medium and used for further experiments. Western blotting and real-time PCR analysis were performed as previously described (Kim et al., 2021). The sequences of the primers used are listed in Table S3.

For TLR2 blocking, the cells were pretreated with anti-human TLR2 antibody (Invivogen, B4H2, 5  $\mu$ g/mL) or isotype control (Invivogen, human IgA2, 5  $\mu$ g/mL) for 1 h. Then, the cells were stimulated with the indicated stimuli for 24 h. The antibodies used for Western blotting and TLR2 blocking are listed in Table S4.

RNA interference assays were performed as previously described (Jun et al., 2018). Briefly, each predesigned siRNA for TLR2 (Invitrogen, HSS186356) and stealth RNAi-negative control duplex (Invitrogen) was transfected into the cells ( $5 \times 10^5$  cells/well in 6-well plates) at a final concentration of 20 nM with Lipofectamine RNAiMAX (Invitrogen) reagent for 24 h. Then, the cells were stimulated with the indicated stimuli for further experiments.

## 2.12 | TLR2-activating assay using HEK-Blue hTLR2 cells

The TLR2-activating ability of human serum was analysed using HEK-Blue hTLR2 cells (Invivogen) according to the manufacturer's instructions. Briefly, the cells ( $5 \times 10^4$  cells/well in 96-well plates) were pretreated with anti-human TLR2 antibody (Invivogen, B4H2, 5  $\mu$ g/mL) or isotype control (Invivogen, human IgA2, 5  $\mu$ g/mL) for 1 h. Then, the cells were treated with 20  $\mu$ L of serum from NAFLD patients or healthy subjects for 24 h. To analyse the TLR2-activating ability of bacterial EVs, the cells were stimulated with the indicated bacterial EVs for 24 h. Secreted embryonic alkaline phosphatase (SEAP) was measured by a spectrophotometer at 655 nm.

## 2.13 | Statistical analysis

All experiments were performed at least three times. The data were analysed using GraphPad Prism 9 software (GraphPad Software Inc., San Diego, CA, USA). Student's *t*-test was used to determine statistical significance between two independent groups. One-way analysis of variance (ANOVA) with Bonferroni's multiple comparison test was used to determine statistical significance among multiple groups with one independent variable. Two-way ANOVA with Bonferroni's multiple comparison test was used to determine statistical significance among multiple groups with two independent variables. Spearman's rank correlation test was used to analyse the data from PAI-1 levels and TLR2-activating ability using human serum. The data are shown as the mean values  $\pm$  standard deviations. A *p* value of <0.05 was considered statistically significant.

# 3 | RESULTS

## 3.1 | *F. alocis* EVs increase PAI-1 expression in the liver

Systemically administered bacterial EVs tend to mainly accumulate in the liver (Jang et al., 2015). To quantify the amount of *F. alocis* EVs (Fa EVs) in the liver after systemic administration, we intraperitoneally injected Fa EVs into mice and measured Fa proteins in the liver using direct ELISA. Fa proteins were detected in mouse livers 1 and 3 h after intraperitoneal injection of Fa EVs (Figure 1a). Next, to investigate the effect of Fa EVs on liver diseases, we intraperitoneally injected Fa EVs and performed a quantitative polymerase chain reaction (qPCR) array for 93 liver cancer-related genes, and the majority of them were also associated with metabolism/steatosis. A heatmap showed the different expression patterns in Fa EV-administered mouse livers compared to control mouse livers, and the top 10 genes that increased 3-fold or more compared to the PBS group are shown (Figure 1b). PAI-1 mRNA was most highly (180.9-fold) increased by Fa EVs, followed by TLR2, intercellular adhesion molecule-1

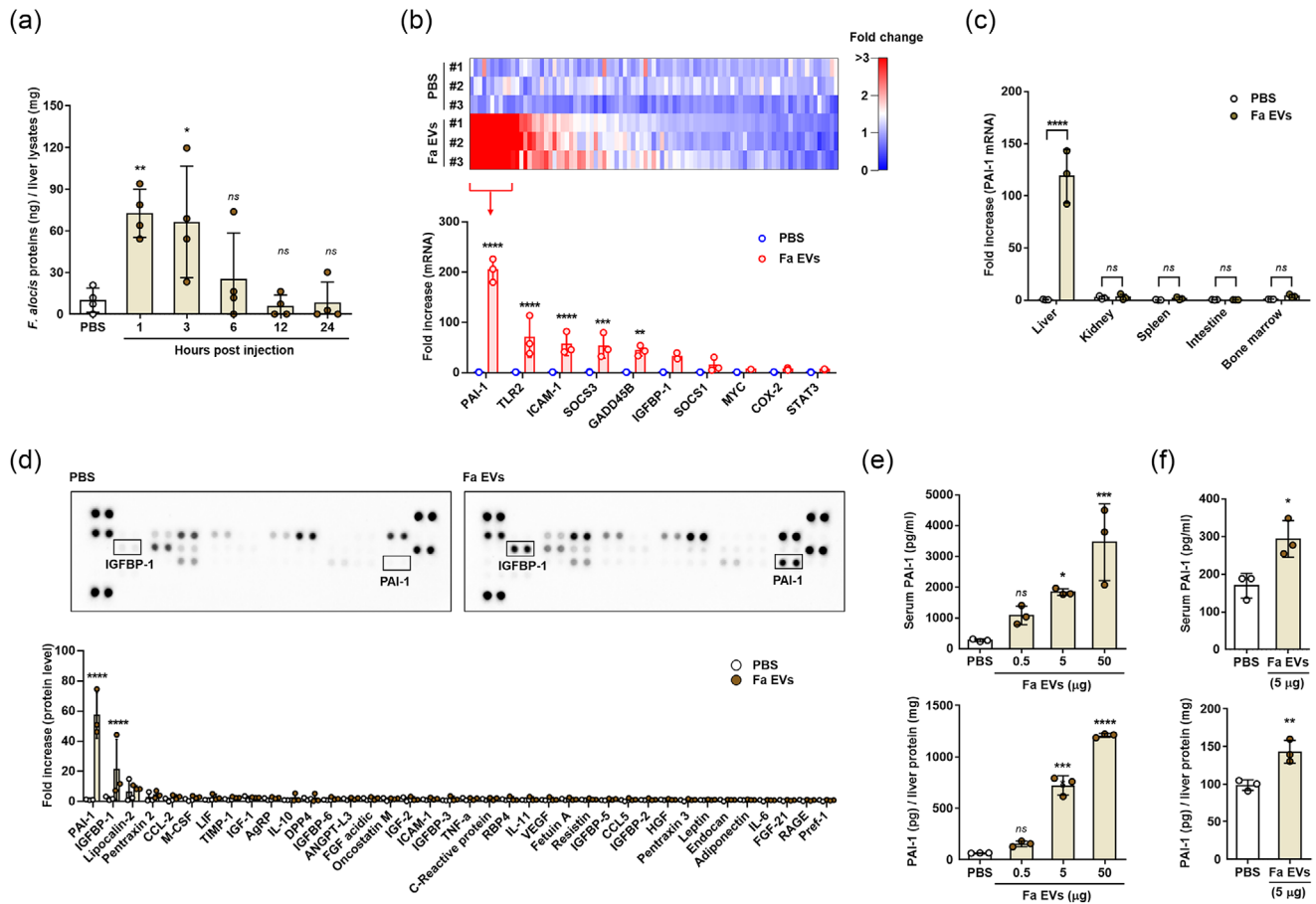


**FIGURE 1** PAI-1 induction by *F. alocis* EVs in mouse livers. (a) Mice ( $n = 4$ ) were administered Fa EVs ( $50 \mu\text{g}$ ) by intraperitoneal injection. After the indicated time periods, the liver was extracted, homogenized with RIPA buffer, and subjected to direct ELISA using anti-*F. alocis* rabbit serum. (b, c) Mice ( $n = 3$ ) were administered Fa EVs ( $50 \mu\text{g}$ ) by intraperitoneal injection. After 1 h, mRNA was extracted from 50 mg of mouse liver, kidney, spleen, and intestine. The mRNA expression levels of 90 liver disease-related genes were analysed by qPCR array (b). PAI-1 mRNA expression levels were analysed by real-time PCR (c). (d) Mice ( $n = 3$ ) were administered Fa EVs ( $50 \mu\text{g}$ ) by intraperitoneal injection. After 3 h, proteins were extracted from mouse livers (100 mg), and liver lysates (500  $\mu\text{g}$ ) were subjected to an adipokine array. A total of 38 obesity-related molecules were analysed by dot blot analysis (upper panel), and the fold increase (lower panel) was determined by densitometry using ImageJ software. (e) Mice ( $n = 3$ ) were intraperitoneally administered Fa EVs (0.5, 5, and 50  $\mu\text{g}$ ) for 3 h. (f) Mice ( $n = 3$ ) were administered Fa EVs (10  $\mu\text{g}/5 \mu\text{L}$ ; 5  $\mu\text{g}$  each in the palate) by palatal injection for 3 h. PAI-1 expression levels in serum and liver lysates were measured using ELISA. The graphs are shown as the mean values  $\pm$  standard deviations. Representative data from three biological replicates are shown. Statistical significance was determined by two-tailed Student's *t* test (f), one-way ANOVA with Bonferroni's multiple comparison test (a, e) or two-way ANOVA with Bonferroni's multiple comparison test (b, c, d). \* $P < 0.05$ , \*\* $P < 0.01$ , \*\*\* $P < 0.001$ , \*\*\*\* $P < 0.0001$  compared to the nontreatment (PBS) group. *ns* denotes not significant.

(ICAM-1), suppressor of cytokine signalling 3 (SOCS3), and growth arrest and DNA-damage-inducible beta (GADD45B). These top five genes that were significantly upregulated by Fa EVs are related to liver steatosis (Fuhrmeister et al., 2016; Henkel et al., 2018; Himes & Smith, 2010; Kono et al., 2001; Xu et al., 2020). Elevated PAI-1 mRNA expression by Fa EVs was observed only in the liver but not in the kidney, spleen, intestine, or bone marrow (Figure 1c). We also analysed the protein expression patterns of 38 molecules by Fa EVs using an adipokine array kit. Fa EVs significantly increased PAI-1 and IGFBP-1 protein levels (Figure 1d). Fa EVs dose-dependently increased PAI-1 expression in both serum and liver (Figure 1e). The dose of Fa EVs was chosen as 5  $\mu\text{g}/\text{injection}$  for subsequent experiments on NAFLD. Upon palatal injection of Fa EVs (total 10  $\mu\text{g}$ ; 5  $\mu\text{g}$  each in the palate), Fa EVs also significantly increased PAI-1 expression in both the liver and serum (Figure 1f). These results suggest that Fa EVs accumulated in the liver and potentially induced PAI-1 expression, which is one of the independent risk factors for NAFLD.

### 3.2 | *F. alocis* EVs cause hepatic steatosis in LFD-fed mice

To determine the effect of Fa EVs on NAFLD progression, 8-week-old male mice were fed a low-fat diet (LFD, 10% fat) or high-fat diet (HFD, 60% fat) for 4 weeks. Then, we injected Fa EVs into LFD-fed mice or HFD-fed mice twice a week for an additional 8 weeks (Figure 2a). Regardless of diet conditions, Fa EVs did not change the body weight of the mice (Figure 2b). After the

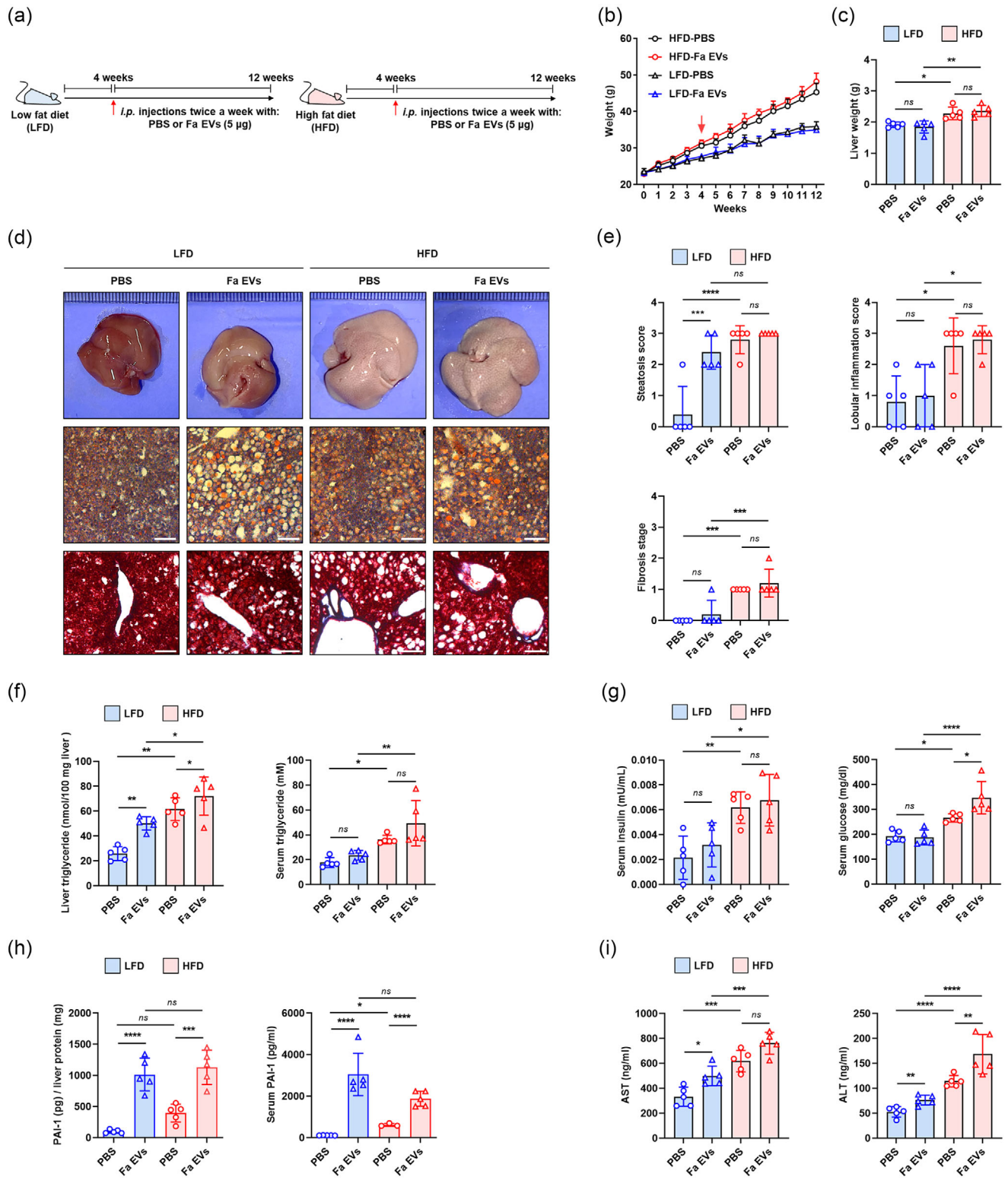


**FIGURE 2** Hepatic steatosis by *F. alocis* EVs in low-fat diet-fed mice. (a) Schematic overview of experimental schemes. (b) Body weight of low-fat diet (LFD, left)-fed or high-fat diet (HFD, right)-fed mice administered PBS- or Fa EVs (twice a week for 8 weeks,  $n = 5$ ). Mice were sacrificed 1 h after the last injection. (c) Liver weight ( $n = 5$ ). (d) Typical pictures of liver (upper), representative images of Oil Red O stained liver sections (middle,  $n = 5$ , Scale bar, 100  $\mu\text{m}$ ), and representative images of trichrome stained liver sections (lower,  $n = 5$ , Scale bar, 100  $\mu\text{m}$ ). (e) Steatosis score, lobular inflammation score, and fibrosis stage of liver sections ( $n = 5$ ). (f) Triglyceride levels in liver tissue and serum ( $n = 5$ ). (g) Insulin and glucose concentrations in mouse serum ( $n = 5$ ). (h) PAI-1 concentration in liver lysates and serum ( $n = 5$ ). (i) Serum AST and ALT levels ( $n = 5$ ). The graphs are shown as the mean values  $\pm$  standard deviations. Statistical significance was determined by two-way ANOVA with Bonferroni's multiple comparison test.  $*P < 0.05$ ,  $**P < 0.01$ ,  $***P < 0.001$ ,  $****P < 0.0001$  compared to the indicated group. *ns* denotes not significant.

experimental period, we injected the mice with Fa EVs for 1 h and sacrificed the mice for the following experiments. Fa EVs did not change liver weight in either LFD- or HFD-fed mice (Figure 2c). Interestingly, gross morphology, histology, steatosis score and triglyceride assay showed that Fa EVs increased hepatic steatosis in LFD-fed mice, but they did not show additional effects on HFD-induced liver steatosis (Figure 2d-f). Histological analysis showed that *F. alocis* EVs did not induce liver inflammation and liver fibrosis in both LFD- and HFD-fed mice (Figure 2d, e). Serum insulin, serum glucose, food intake, subcutaneous fat, and visceral fat were not altered by Fa EVs in LFD-fed mice (Figure 2g, Figure S1a and b). In HFD-fed mice, subcutaneous fat and visceral fat were slightly increased by Fa EVs (Figure S1b). In both LFD- and HFD-fed mice, Fa EVs potentially increased PAI-1 levels in the liver and serum (Figure 2h). PAI-1 levels in the liver exhibited an increasing tendency in the HFD-fed mice compared to the LFD-PBS group (*p* value by Student's *t*-test: 0.0019 for liver PAI-1; *p* value by two-way ANOVA: 0.1403 for liver PAI-1). Fa EVs increased serum AST and ALT levels in both LFD- and HFD-fed mice (Figure 2i). These results suggest that Fa EVs can cause hepatic steatosis and increase PAI-1 expression even in LFD-fed mice.

### 3.3 | PAI-1 inhibition alleviates periodontal pathogen EV-induced hepatic steatosis

To identify the role of PAI-1 in EV-induced hepatic steatosis, we examined the effects of TM5441, a pharmacological inhibitor of PAI-1 (Henkel et al., 2018; Lee et al., 2017), on periodontal pathogen EV-induced hepatic steatosis. Eight-week-old male mice were fed the LFD for 4 weeks. Then, we injected LFD-fed mice with periodontal pathogen EVs and TM5441 twice a week for 8 weeks (Figure 3a). Pharmacological perturbation of PAI-1 did not affect the body weight or food intake of the mice (Figures 3b and S2). To test whether PAI-1 is inhibited by TM5441, a PAI-1 activity assay was performed. As shown in Figure 3c, Fa EVs and *P. gingivalis* EVs (Pg EVs) significantly increased the active PAI-1 level in vehicle control mice, and the active PAI-1 level was decreased in TM5441-treated mice to the control level. Gross morphology and histology data showed that TM5441 alleviated hepatic steatosis induced by Fa EVs or Pg EVs but did not affect liver weight (Figure 3d-f). PAI-1 inhibition alleviated the induction of liver triglyceride levels by Fa EVs or Pg EVs (Figure 3g). PAI-1 levels are known to affect the gene expression levels of hepatic enzymes involved in triglyceride synthesis (Henkel et al., 2018; Levine et al., 2021). Consistent with the histology and triglyceride analysis results, periodontal pathogen EVs induced the expression of triglyceride synthesis-related hepatic genes (SREBP-1c, FAS, and ACC), which were decreased by TM5441 treatment (Figure 3h). Next, we tested the effects of PAI-1 inhibition on serum AST/ALT levels. PAI-1 inhibition by TM5441 did not affect blood AST levels increased by periodontal pathogen EVs (Figure 3i). Increased serum ALT levels by Fa EVs were slightly decreased by TM5441 treatment, but ALT levels by Pg EVs were not affected. It was reported that TM5441 treatment decreased plasma ALT levels in standard fat diet-fed mice at 8 weeks but not at 16 weeks (Henkel et al., 2018). These results suggest that PAI-1 is a key molecule in hepatic steatosis caused by periodontal pathogen EVs.

### 3.4 | TLR2 regulates periodontal pathogen EV-induced PAI-1 expression and hepatic steatosis

TLR signalling by bacterial MAMPs is associated with NAFLD progression (Miura & Ohnishi, 2014). Recently, we reported that EVs from periodontal pathogens, including *F. alocis*, *P. gingivalis*, and *T. forsythia*, preferentially activated TLR2 rather than TLR4 and TLR9 (Kim et al., 2022). We therefore investigated the role of TLR2 in periodontal pathogen EV-induced liver steatosis. Eight-week-old WT or TLR2<sup>-/-</sup> male mice were fed a ND for 4 weeks. Then, we injected the mice with periodontal pathogen EVs (Fa EVs or Pg EVs) twice a week for 8 weeks (Figure 4a). Compared to WT mice, TLR2<sup>-/-</sup> mice showed reduced body weight gain (Figure 4b). TLR2<sup>-/-</sup> mice also showed reduced liver weight in the Fa EV-administered group but not in the PBS- or Pg EV-administered group (Figure 4c). Food intake did not change (Figure S3a). Interestingly, the steatosis score and liver triglyceride levels were not increased by periodontal pathogen EVs in TLR2<sup>-/-</sup> mice (Figure 4d-f). PAI-1 expression was not induced by EVs in either the liver or serum of TLR2<sup>-/-</sup> mice (Figure 4g). Accordingly, the expression of SREBP-1c, FAS, and ACC was not induced by EVs in the livers of TLR2<sup>-/-</sup> mice (Figure 4h). Fa EVs and Pg EVs did not increase either AST or ALT levels in TLR2<sup>-/-</sup> mice (Figure 4i). These results suggest that TLR2 is an important receptor for periodontal pathogen EV-induced liver steatosis and PAI-1 induction.

Proinflammatory cytokines, such as IL-1, IL-6, and TNF- $\alpha$ , are known to activate hepatocytes to induce PAI-1 expression (Dimova & Kietzmann, 2008). IL-6 levels were increased in the serum of WT mice by periodontal pathogen EVs, whereas they were not induced in TLR2<sup>-/-</sup> mice. In liver lysates, periodontal pathogen EVs did not increase IL-6 levels, and the IL-6 levels were not different between WT and TLR2<sup>-/-</sup> mice (Figure S3b). These results suggest that periodontal pathogen EVs may directly induce PAI-1 via TLR2 independently of signalling pathways by proinflammatory cytokines.

### 3.5 | PAI-1 levels are correlated with TLR2-activating ability in human serum

EVs may circulate in the bloodstream and activate TLR2 to induce PAI-1. To determine the correlation between TLR2-activating ability and PAI-1 levels in humans, we prepared serum from NAFLD patients (*n* = 100) and healthy subjects (*n* = 100). To



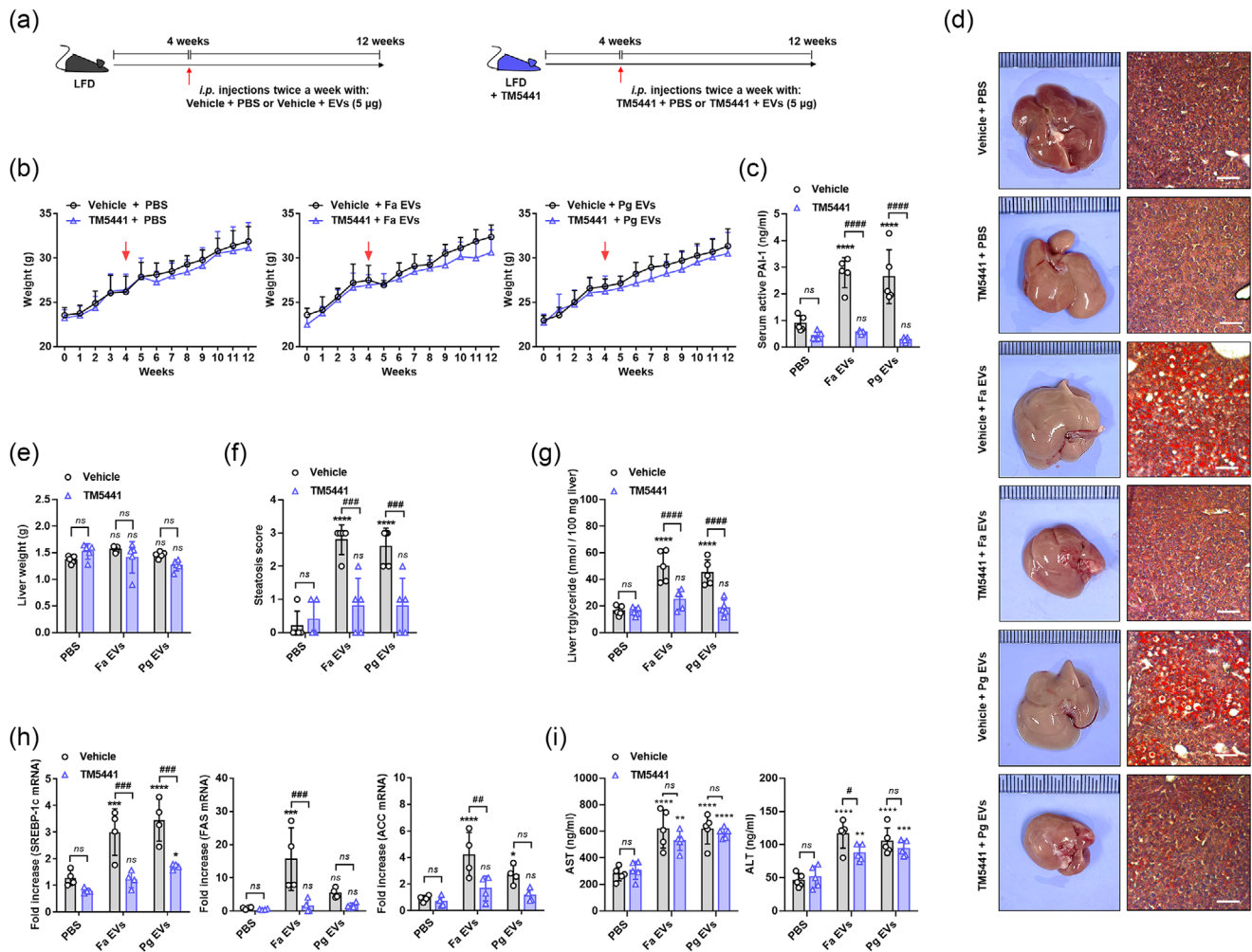


**FIGURE 3** Effects of pharmacological inhibition of PAI-1 on EV-induced steatosis. (a) Schematic overview of experimental schemes. (b) Body weight of LFD-fed mice administered PBS, Fa EVs, or Pg EVs (twice a week for 8 weeks) in the presence or absence of TM5441 injection (20 mg/kg,  $n = 5$ ). (c) Serum active PAI-1 levels were measured using an active PAI-1 ELISA kit. (d) Typical pictures of liver and representative images of Oil Red O stained liver sections ( $n = 5$ , Scale bar, 100  $\mu\text{m}$ ). (e) Liver weight ( $n = 5$ ) and (f) steatosis score of liver sections ( $n = 5$ ). (g) Triglyceride levels in liver tissue ( $n = 5$ ). (h) Gene expression levels of SREBP-1c, FAS, and ACC in the liver ( $n = 5$ ). (i) Serum AST and ALT levels ( $n = 5$ ). The graphs are shown as the mean values  $\pm$  standard deviations. Statistical significance was determined by two-way ANOVA with Bonferroni's multiple comparison test. \* $P < 0.05$ , \*\* $P < 0.01$ , \*\*\* $P < 0.001$ , \*\*\*\* $P < 0.0001$  compared to each PBS group. ## $P < 0.01$ , ### $P < 0.001$ , #### $P < 0.0001$  compared to the indicated group. *ns* denotes not significant.

analyse whether TLR2 ligands are increased in NAFLD patients, we used a TLR2 reporter cell line, HEK-Blue hTLR2 cells, to measure the TLR2-activating ability of serum. Interestingly, the ability of serum from NAFLD patients to activate TLR2 was higher than that from healthy subjects (Figure 5a). To exclude the possibility of other contaminants that may activate the cells via TLR2, we used anti-hTLR2 IgA. The blocking of TLR2 with a neutralizing antibody downregulated the TLR2-activating ability of serum from both NAFLD patients and healthy subjects. Pam3CSK4, a TLR2 ligand, was used as a control for the TLR2 blocking antibody (Figure 5b). We also measured serum PAI-1 levels in NAFLD patients and healthy subjects. As expected, PAI-1 was elevated in serum from NAFLD patients (Figure 5c). The concentration of PAI-1 in serum exhibited a significant moderate positive correlation with the TLR2-activating ability of serum ( $r = 0.4233$ ,  $p < 0.0001$ , Figure 5d). Furthermore, serum from NAFLD patients contain more amount of *F. alocis* proteins and *P. gingivalis* proteins than serum from healthy subjects (Figure 5e, h). The concentration of *F. alocis* protein and *P. gingivalis* protein in the serum were positively correlated with the serum PAI-1 concentration, and they also exhibited a positive correlation with the TLR2-activating ability (Figure 5f, g, i, j). Collectively, these results indicate that circulating TLR2 ligands, such as periodontal pathogen proteins are increased in the serum from NAFLD patients and contribute to stimulating the liver to express PAI-1.

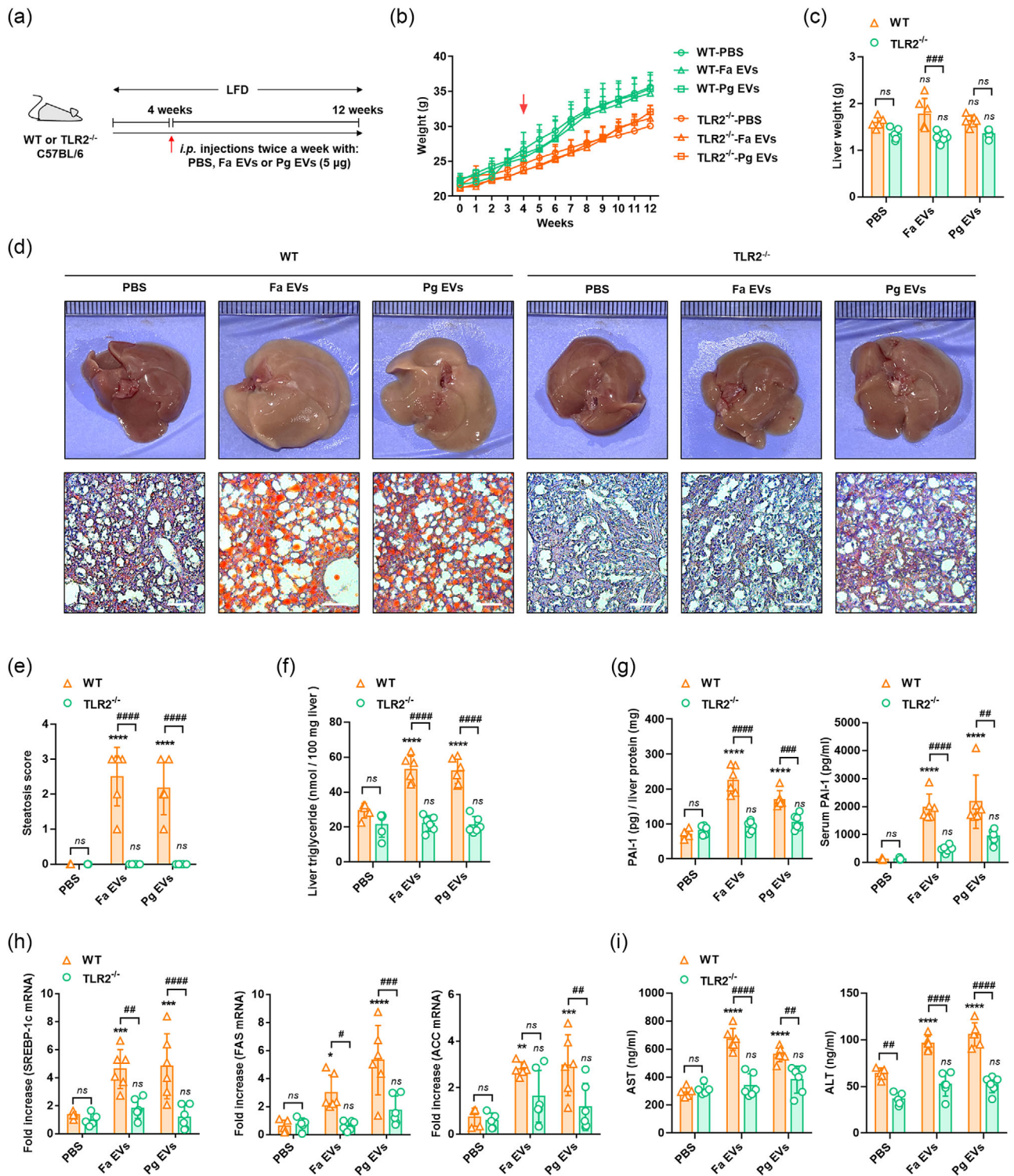


**FIGURE 4** Role of TLR2 in periodontal pathogen EV-induced liver steatosis. (a) Schematic overview of experimental schemes. (b) Body weight of LFD-fed WT or TLR2<sup>-/-</sup> mice administered PBS, Fa EVs, or Pg EVs (twice a week for 8 weeks,  $n = 5$  for PBS groups;  $n = 6$  for Fa EV and Pg EV groups). Mice were sacrificed 1 h after the last injection. (c) Liver weight ( $n = 5$  for PBS groups;  $n = 6$  for Fa EV and Pg EV groups). (d) Typical pictures of liver (upper) and representative image of Oil Red O stained liver sections (lower,  $n = 5$  for PBS groups;  $n = 6$  for Fa EV and Pg EV groups, Scale bar, 100 μm). (e) Steatosis score of liver sections ( $n = 5$  for PBS groups;  $n = 6$  for Fa EV and Pg EV groups). (f) Triglyceride levels in liver tissue ( $n = 5$  for PBS groups;  $n = 6$  for Fa EV and Pg EV groups). (g) PAI-1 concentration in liver lysates and serum ( $n = 5$  for PBS groups;  $n = 6$  for Fa EV and Pg EV groups). (h) Gene expression levels of SREBP-1c, FAS, and ACC in the liver ( $n = 5$  for PBS groups;  $n = 6$  for Fa EV and Pg EV groups). (i) Serum AST and ALT levels ( $n = 5$  for PBS groups;  $n = 6$  for Fa EV and Pg EV groups). The graphs are shown as the mean values  $\pm$  standard deviations. Statistical significance was determined by two-way ANOVA with Bonferroni's multiple comparison test. \* $P < 0.05$ , \*\* $P < 0.01$ , \*\*\* $P < 0.001$ , \*\*\*\* $P < 0.0001$  compared to the PBS group. # $P < 0.05$ , ## $P < 0.01$ , ### $P < 0.001$ , #### $P < 0.0001$  compared to the indicated group. ns denotes not significant.

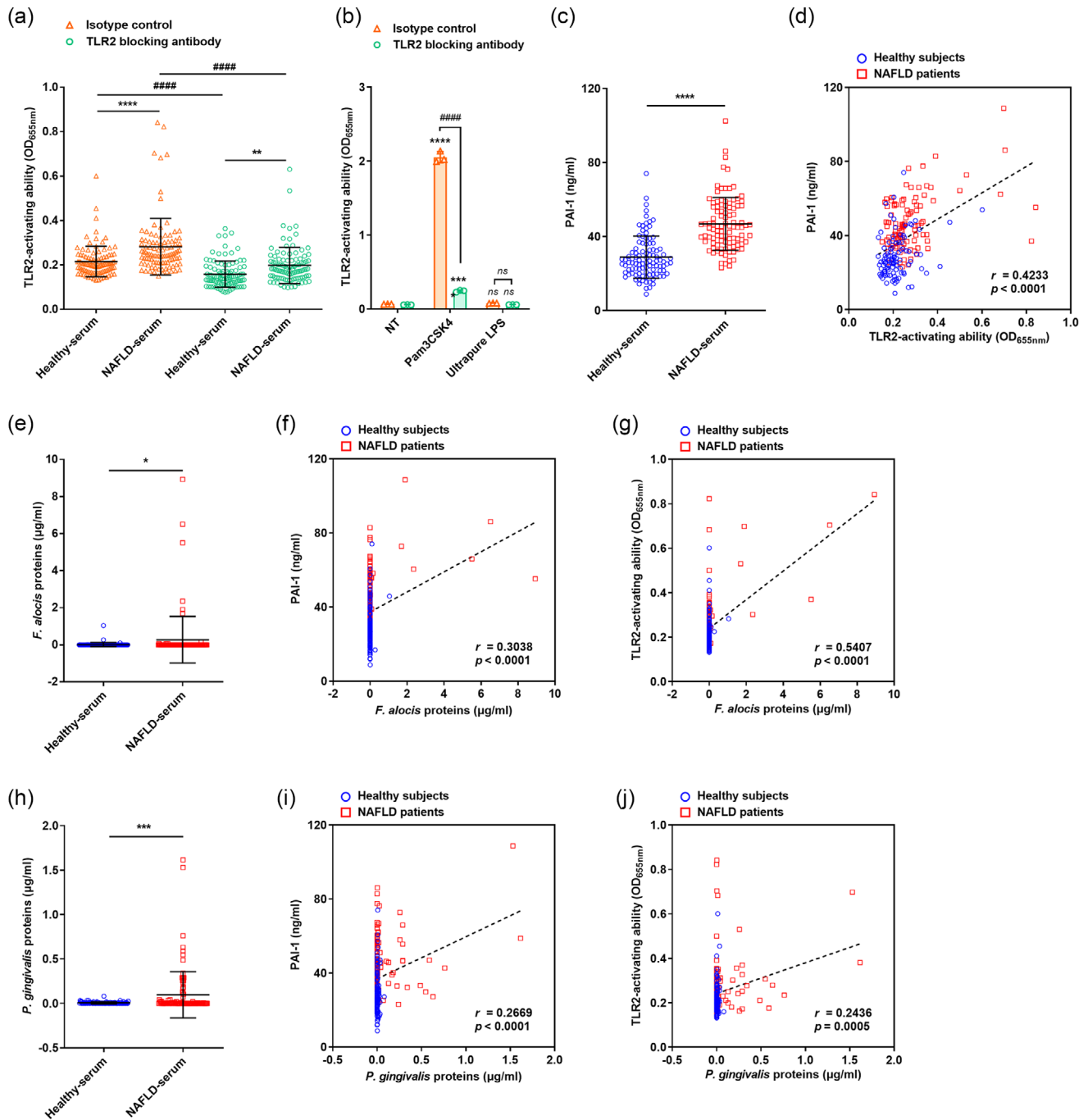


**FIGURE 5** PAI-1 levels, TLR2-activating ability, and periodontal pathogen proteins of serum from NAFLD patients. (a, b) HEK-Blue hTLR2 cells ( $5 \times 10^4$  cells/well in 96-well plates) were pretreated with  $5 \mu\text{g}/\text{mL}$  anti-hTLR2 IgA or isotype human IgA2 for 1 h. Then, the cells were treated with  $20 \mu\text{L}$  of serum from healthy subjects ( $n = 100$ ) or NAFLD patients ( $n = 100$ ) for an additional 20 h (a). Pam3CSK4 (100 ng/mL) and ultrapure LPS (100 ng/mL) were used as controls for the TLR2 ligand and TLR4 ligand, respectively (b). The TLR2-activating ability of serum was measured by SEAP assay using a spectrophotometer. (c) PAI-1 levels in serum from healthy subjects ( $n = 100$ ) or NAFLD patients ( $n = 100$ ) were measured by ELISA. (d) Correlation plot between the PAI-1 levels in human serum and the TLR2-activating ability of human serum. (e) Concentration of *F. alocis* proteins in human serum were measured using an anti-*F. alocis* rabbit serum. (f) Correlation plot between the PAI-1 levels in human serum and the *F. alocis* protein concentration of human serum. (g) Correlation plot between the TLR2-activating ability of human serum and the *F. alocis* protein concentration of human serum. (h) Concentration of *P. gingivalis* proteins in human serum were measured using an anti-*P. gingivalis* monoclonal antibody. (i) Correlation plot between the PAI-1 levels in human serum and the *P. gingivalis* protein concentration of human serum. (j) Correlation plot between the TLR2-activating ability of human serum and the *P. gingivalis* protein concentration of human serum. Statistical significance was determined by two-tailed Student's *t* test (a, b, e, h), two-way ANOVA with Bonferroni's multiple comparison test (c), or Spearman's rank correlation test (d, f, g, i, j). \* $P < 0.05$ , \*\* $P < 0.01$ , \*\*\*\* $P < 0.0001$  compared to the serum from healthy subjects. ####  $P < 0.0001$  compared to the indicated group. *ns* denotes not significant.

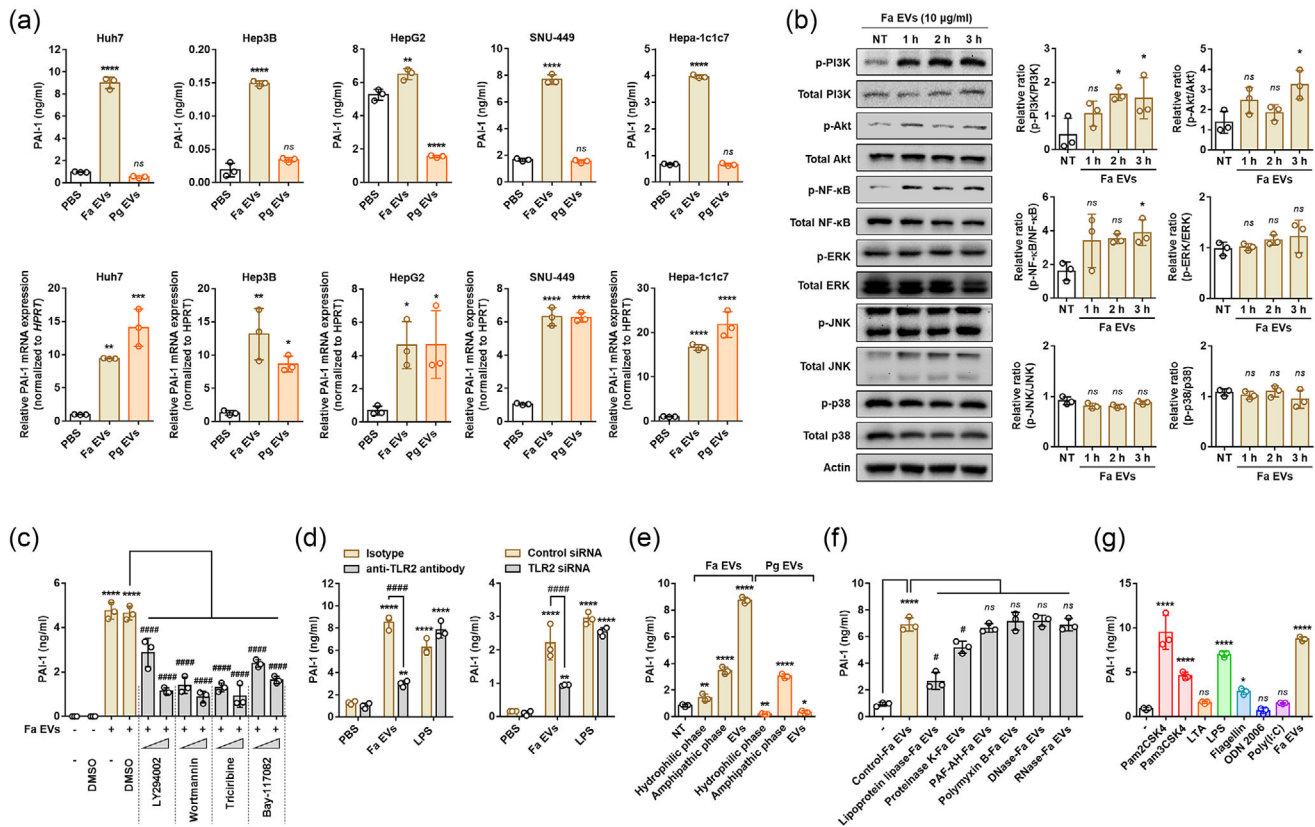


**FIGURE 6** PAI-1 induction by periodontal pathogen EVs in hepatocytes. (a) Hepatocyte cell lines ( $2 \times 10^5$  cells in 48-well plates for ELISA,  $4 \times 10^5$  cells in 6-well plates for RT-PCR) were stimulated with  $10 \mu\text{g}/\text{mL}$  indicated stimuli for 24 h (ELISA) or for 3 h (RT-PCR). PAI-1 expression at the protein level (upper panel) and mRNA level (lower panel) was analysed by ELISA and RT-PCR, respectively. (b) Huh7 cells ( $4 \times 10^5$  cells in 6-well plates) were stimulated with  $10 \mu\text{g}/\text{mL}$  of Fa EVs for 1, 2, or 3 h. Phosphorylation of each molecule was determined by Western blotting. Band intensities in the Western blots were quantified by densitometry using ImageJ software and presented as the relative ratio to the total form of each signalling molecule. (c) Huh7 cells ( $2 \times 10^5$  cells in 48-well plates) were pretreated with the indicated inhibitors (1 or  $10 \mu\text{M}$ ) for 1 h. Then, the cells were stimulated with  $10 \mu\text{g}/\text{mL}$  of Fa EVs for 24 h. (d) Huh7 cells ( $2 \times 10^5$  cells in 48-well plates) were pretreated with TLR2-blocking antibody or isotype control for 1 h and stimulated with the indicated stimuli (left panel). Huh7 cells ( $4 \times 10^5$  cells in 6-well plates) were transfected with TLR2 siRNA for 18 h and stimulated with  $10 \mu\text{g}/\text{mL}$  of Fa EVs for 3 h (right panel). (e, f, g) Huh7 cells ( $2 \times 10^5$  cells in 48-well plates) were stimulated with the indicated stimuli ( $10 \mu\text{g}/\text{mL}$ ) for 24 h. PAI-1 protein levels in the cell culture supernatants were analysed by ELISA (c, d, e, f, g). \* $P < 0.05$ , \*\* $P < 0.01$ , \*\*\* $P < 0.001$ , \*\*\*\* $P < 0.0001$  compared to the PBS group. # $P < 0.05$ , #### $P < 0.0001$  compared to the indicated group. ns denotes not significant.

### 3.6 | Periodontal pathogen EVs induce PAI-1 expression via TLR2-PI3K-Akt-NF- $\kappa$ B in hepatocytes

Hepatocytes, the most abundant cell type in the liver, are one of the main populations expressing PAI-1 (MacParland et al., 2018). To test PAI-1 expression by periodontal pathogen EVs in hepatocytes, we used both human hepatocytes (Huh7, Hep3B, SNU-449, and HepG2) and mouse hepatocytes (Hepa-1c1c7). As shown in Figure 6a, Fa EVs increased PAI-1 expression at both the protein (upper panel) and mRNA levels (lower panel) in hepatocytes. Pg EVs increased PAI-1 mRNA but not PAI-1 protein. In HepG2 cells, Pg EVs even decreased PAI-1 protein. This might be due to gingipains, proteases that can degrade the PAI-1 protein *in vitro* (Song et al., 2021). To identify whether gingipains degrade PAI-1 induced by Pg EVs, we prepared EVs from gingipain-deficient *P. gingivalis* (KDPI36). Gingipain-deficient *P. gingivalis* EVs (KDPI36) but not WT Pg EVs increased PAI-1 protein in Huh7 cells (Figure S4). These results indicate that Fa EVs and Pg EVs can efficiently increase PAI-1 expression in hepatocytes, although Pg EV-induced PAI-1 can be degraded by gingipains present in Pg EVs.

To determine the role of EVs from different bacteria in PAI-1 induction, we used EVs from another periodontal pathogen, *T. forsythia*, an oral commensal strain, *Streptococcus oralis*, and a gut probiotic strain, *Lactobacillus reuteri*. EVs from *T. forsythia* (Tf EVs) and EVs from *S. oralis* (So EVs) significantly increased PAI-1 expression both *in vivo* and *in vitro* (Figure S5a, b). EVs from *L. reuteri* (Lr EVs) did not induce PAI-1 induction *in vivo* and slightly induced PAI-1 in mouse hepatocytes.

The PI3K/Akt, NF- $\kappa$ B, and MAPK pathways are involved in PAI-1 expression in hepatocytes and are activated by TLR signalling pathways (Dimova & Kietzmann, 2008). To confirm that periodontal pathogen EVs can activate signalling molecules, Huh7 cells were stimulated with Fa EVs. Fa EVs significantly induced the phosphorylation of PI3K, Akt, and NF- $\kappa$ B but not MAPK (Figure 6b). PAI-1 induction by Fa EVs was attenuated by PI3K inhibitors (LY294002 and wortmannin), an Akt inhibitor

(tricyribine), and an NF- $\kappa$ B inhibitor (Bay-117082) without cell death (Figures 6c and S6a). The effects of wortmannin and tricyribine on the inhibition of PI3K were confirmed by Western blotting (Figure S6b). Next, to examine the effects of TLR2 on Fa EV-induced PAI-1 induction in hepatocytes, we used a TLR2 blocking antibody and TLR2 siRNA. As shown in Figure 6d, blocking or knock down TLR2 significantly attenuated Fa EV-induced PAI-1 induction in hepatocytes. LPS, a TLR4 ligand, was used as a negative control for TLR2 blocking or knockdown.

Previously, we demonstrated that amphiphilic molecules of Fa EVs are essential for inducing TLR2 activation (Kim et al., 2021). To identify the role of amphiphilic molecules of Fa EVs and Pg EVs in PAI-1 induction, we separated the EVs into an amphiphilic phase and a hydrophilic phase. As expected, the amphiphilic phase from Fa EVs highly induced PAI-1 induction, but the hydrophilic phase of Fa EVs was slightly induced (Figure 6e). Interestingly, the Pg EV-derived hydrophilic phase decreased PAI-1 expression levels, as shown with Pg EVs, but the amphiphilic phase from Pg EVs significantly induced PAI-1 levels in hepatocytes. To investigate the role of MAMPs from Fa EVs, we treated Fa EVs with various MAMP inhibitors (lipoprotein lipase and proteinase K for bacterial lipoproteins, PAF-AH for LTA, polymyxin B for endotoxin, DNase for DNA, and RNase for RNA). As shown in Figure 6f, lipoprotein inhibitors attenuated PAI-1 induction by Fa EVs. We further examined the role of various TLR ligands in PAI-1 induction in hepatocytes. Pam2CSK4 (TLR2/6 ligand), Pam3CSK4 (TLR1/2 ligand), LPS (TLR4 ligand), and flagellin (TLR5 ligand) significantly induced PAI-1 expression in hepatocytes, while LTA (TLR2 ligand), ODN 2006 (TLR9 ligand), and poly (I:C) did not induce PAI-1 expression (Figure 6g). These results suggest that bacterial lipoproteins, as TLR2 ligands in periodontal pathogen-derived EVs, are key players in the induction of PAI-1 in hepatocytes.

## 4 | DISCUSSION

NAFLD progression is affected by microbiota in various ways, including microbiota dysbiosis, microbial infection, microbial metabolites, and endotoxaemia (Aron-Wisniewsky et al., 2020). Recently, the oral-gut-liver axis has gained attention for understanding the molecular mechanisms of liver diseases or intestinal diseases in periodontitis patients (Acharya et al., 2017; Chen et al., 2023; Wang et al., 2022). Periodontal pathogens affect systemic diseases, including NAFLD, and are more frequently found in liver biopsies from NAFLD patients than healthy individuals (Akinkugbe et al., 2017; Helenius-Hietala et al., 2019; Komazaki et al., 2017; Yoneda et al., 2012). Bacterial EVs can accumulate in the liver by circulating throughout the whole body (Jang et al., 2015). In the present study, we showed that low-dose periodontal pathogen EVs directly increased PAI-1 levels in livers from LFD mice through TLR2 signalling, resulting in liver steatosis. PAI-1 levels were higher in serum from NAFLD patients than in serum from healthy controls, and serum PAI-1 levels showed a positive correlation with serum TLR2-activating ability. Fa EVs increased PAI-1 in hepatocytes through TLR2 with the PI3K/Akt/NF- $\kappa$ B signalling pathway. This is the first study of the role of the interaction between periodontal pathogen EVs and the TLR2/PAI-1 axis in NAFLD progression.

Here, we determined that long-term exposure to low-dose EVs from both gram-negative and gram-positive periodontal pathogens induced hepatic steatosis in LFD mice. Similar to our study, Seyama *et al.* demonstrated that *P. gingivalis* EVs transferred their gingipains to the liver, leading to the progression of diabetes mellitus symptoms by inhibiting insulin signalling in hepatocytes (Seyama et al., 2020). The effects of bacterial EVs on liver diseases are diverse depending on the bacterial species. Zahmatkesh et al. suggested that EVs from *Helicobacter pylori*, a gastrointestinal pathogen, may induce liver fibrosis through the induction of liver fibrosis markers, including  $\alpha$ -SMA, TIMP-1,  $\beta$ -catenin, and vimentin, in hepatic stellate cells (Zahmatkesh et al., 2022). EVs from *Akkermansia muciniphila*, a next-generation probiotic strain, have anti-inflammatory abilities in both HFD- and carbon tetrachloride-induced liver injury mice (Raftar et al., 2022). EVs from *Lactobacillus rhamnosus* GG, a probiotic strain, alleviated alcohol-associated liver disease progression by enhancing intestinal barrier functions (Gu et al., 2021). We also showed that EVs from *L. reuteri*, a probiotic strain, did not induce PAI-1 expression, but EVs from *T. forsythia*, a periodontal pathogen, and *S. oralis*, an oral commensal strain, induced PAI-1. Although we identified the role of EVs from *F. alocis* and *P. gingivalis* as representative periodontal pathogens in NAFLD progression, further studies are needed to determine the overall effects of oral microbiome-derived EVs on liver diseases.

We showed that serum from NAFLD patients contained significantly higher PAI-1 levels than serum from healthy individuals. PAI-1 is an important regulator of lipid metabolism in the liver. PAI-1 inhibitors can downregulate the mRNA expression of lipid synthesis-related genes, including SREBP, in the livers of high fat/high cholesterol high sugar (HFHS)-fed mice (Levine et al., 2021). PAI-1 knockout mice are resistant to HFHS-induced hepatic steatosis, and administration of a PAI-1 inhibitor alleviates HFHS-induced hepatic steatosis (Henkel et al., 2018). The authors suggested that genetic knockout of PAI-1 and PAI-1 inhibitor did not prevent hepatic inflammation and fibrosis by HFHS- or methionine- and choline-deficient diet-induced NAFLD mouse model. However, Lee et al. suggested that a PAI-1 inhibitor can not only alleviate HFD-induced hepatic steatosis but also alleviate both hepatic inflammation and fibrosis in HFD mice (Lee et al., 2017). In our study, periodontal pathogen EVs potently increased PAI-1 induction in liver and hepatic steatosis but not hepatic inflammation and fibrosis in LFD mice. Hepatic steatosis and lipid synthesis-related genes (SREBP-1c, FAS, and ACC) induced by periodontal pathogen EVs were decreased by a PAI-1 inhibitor. The potential downstream targets of increased PAI-1 in relation to lipid metabolism are as follows: (1) PAI-1 inhibits hepatocyte growth factor (HGF)-induced c-Met pathway, which can export triglycerides and low-density lipoprotein from the

liver by activating microsomal triglyceride transfer protein (MTTP) and apolipoprotein B (Kanuri et al., 2011; Naldini et al., 1995). (2) Inhibition of PAI-1 by PAI-1 inhibitor, TM5614, downregulates plasma level of proprotein convertase subtilisin/kexin type 9 (PCSK9), thereby lowering lipid synthesis in the liver. PCSK has the ability to catabolize LDL receptor, which are crucial for the uptake of cholesterol in the liver, leading to the downregulation of lipid metabolism-related genes such as *Srebp1/2* and *HMG-CoA reductase* (Levine et al., 2021). (3) PAI-1 may inhibit insulin signalling by binding to insulin receptor in hepatocyte, considering that PAI-1 can inhibit insulin signalling by binding  $\alpha\beta 3$  integrin in fibroblasts (Lopez-Aleman et al., 2003). PAI-1 has been shown to be elevated in severe periodontitis patients compared to healthy controls (Bizzarro et al., 2007). Although the role of PAI-1 in hepatic inflammation and fibrosis is controversial, it seems clear that PAI-1 is an important molecule in hepatic steatosis by periodontal pathogen EVs.

In NAFLD/NASH research, TLRs have gained attention due to their roles in interactions with microbiota in our body (Miura & Ohnishi, 2014). A role of TLR-MAMP interactions has been suggested in NAFLD progression. In TLR2<sup>-/-</sup> mice, NASH progression induced by a choline-deficient amino acid-defined (CDAA) diet was alleviated compared to that in WT mice, and Pam3CSK4, a bacterial TLR2 ligand, and CpG-ODN, a bacterial TLR9 ligand, synergistically induced inflammasome activation in liver macrophages (Miura et al., 2012). NAFLD/NASH patients had more LPS in both serum and liver tissue than non-NAFLD subjects (Carpino et al., 2020). Exposure to low-dose LPS exacerbated NASH progression via CD14/STAT3 signalling in HFD mice, and hepatic CD14 expression levels were higher in NAFLD patients than in healthy controls (Imajo et al., 2012). CD14 is known as an essential coreceptor for activating TLRs, including TLR2 and TLR4 (Lee et al., 2012). Endotoxemia induced by sonicated *P. gingivalis* increased liver steatosis in HFD mice (Sasaki et al., 2018). *P. gingivalis* LPS reached the liver by palatal injection and induced NAFLD progression in both LFD and HFD mice (Fujita et al., 2018). Previously, we showed that EVs from gram-negative periodontal pathogens (*P. gingivalis* and *T. forsythia*) contained both bacterial lipoproteins and LPS, and EVs from a gram-positive periodontal pathogen (*F. alocis*) contained lipoproteins (Kim et al., 2021, 2022). EVs from both gram-negative and gram-positive periodontal pathogens mainly activate TLR2 rather than TLR4 (Kim et al., 2022). In this study, TLR2<sup>-/-</sup> mice did not show hepatic steatosis or PAI-1 induction by periodontal pathogen EVs. An *in vitro* study confirmed that TLR2 was important for PAI-1 induction by Fa EVs in hepatocytes. Amphiphilic molecules but not hydrophilic molecules from periodontal pathogen EVs potently increased PAI-1 in hepatocytes. EV inhibition experiments demonstrated that treatment of EVs with lipoprotein lipase and proteinase K decreased PAI-1 induction, whereas treatment with PAF-AH, polymyxin B, DNase and RNase did not. In addition, our data on clinical samples showed that serum from NAFLD patients had a stronger TLR2-activating ability than that from healthy subjects, and serum PAI-1 levels were positively correlated with the TLR2-activating ability of serum. Considering this, in the subgingival sites of periodontitis patients, periodontal pathogens continuously release EVs that transfer their TLR2 ligands, such as bacterial lipoproteins, to the liver, leading to PAI-1 induction and liver steatosis. Although the exact role of the various molecules of periodontal pathogen EVs in NAFLD progression needs to be further elucidated, TLR2-activating molecules such as bacterial lipoproteins may be important for PAI-1 induction leading to NAFLD progression.

In the present study, long-term exposure to low-dose periodontal pathogen EVs increased steatosis and triglyceride levels in livers from LFD-fed mice, but there was no change in body weight, liver weight, and food uptake. Although NAFLD is usually related to metabolic disorders such as obesity, a recent meta-analysis suggested that among all NAFLD patients, approximately 19.2% were lean and 40.8% were nonobese subjects (Ye et al., 2020). Microbiota might be involved in this phenomenon considering that nonobese/lean NAFLD patients have distinct microbiome signatures from obese NAFLD patients in both stool and liver biopsy samples (Duarte et al., 2018; Lee et al., 2020; Suppli et al., 2021). Furthermore, obese NAFLD patients contained more 16S ribosomal DNA in liver samples than lean NAFLD patients, suggesting that translocation of bacteria from the gut to the liver by intestinal inflammation is important for NAFLD progression in obese subjects (Henao-Mejia et al., 2012; Luther et al., 2015). Unlike bacterial cells, bacterial EVs released from microbiota such as gut microbiota and oral microbiota move freely in the circulation and readily penetrate host tissues or biological barriers. The present study indicates that periodontal pathogen EVs can reach the liver and induce PAI-1 induction, leading to hepatic steatosis regardless of metabolic abnormalities.

The increase in hepatic steatosis caused by Fa EVs was only observed under LFD conditions, not in HFD conditions. The increased level of PAI-1 in liver induced by Fa EVs was similar in both LFD and HFD conditions, indicating a plateau in PAI-1 levels. Furthermore, in HFD, there are various other factors that have a significant impact on steatosis: (1) HFD can cause obesity and insulin resistance/hyperinsulinemia, leading to increase in lipogenesis in the liver (Uttschneider & Kahn, 2006). We demonstrated that HFD induced body weight gain and increased levels of serum insulin and glucose, which were not observed under LFD conditions. (2) HFD also causes dysfunction of hepatic autophagy, which can induce insulin resistance and endoplasmic reticulum stress, ultimately leading to hepatic steatosis (Yang et al., 2010). (3) The lipid content of exosomes from HFD-fed mice is different from that of control diet-fed mice (Kumar et al., 2021). Compared to exosomes derived from control diet-fed mice, exosomes from HFD-fed obese mice showed an increase in the phosphatidylcholine (PC) ratio, and PC induced insulin resistance and glucose intolerance through the aryl hydrocarbon receptor, leading to hepatic steatosis. Therefore, we believed that the effects of PAI-1 induction by Fa EVs on liver steatosis might be obscured in HFD conditions, and the PAI-1-mediated hepatic steatosis by periodontal pathogen EVs might play a crucial role in the early stages of NAFLD progression and lean NAFLD.

In summary, we showed that periodontal pathogen-derived EVs increased PAI-1 induction by TLR2 signalling, resulting in hepatic steatosis. We also found that the PAI-1 levels and TLR2-activating ability of NAFLD patient serum were higher than those

of healthy control serum. There was a significant correlation between human serum PAI-1 levels and the TLR2-activating ability of human serum. These results suggested that the TLR2/PAI-1 axis could be a novel molecular mechanism for the association between periodontitis and NAFLD and a potential therapeutic target for NAFLD progression.

## AUTHOR CONTRIBUTIONS

**Hyun Young Kim:** Conceptualization (lead); data curation (equal); funding acquisition (lead); formal analysis (lead); investigation (lead); methodology (lead); validation (lead); writing—original draft (lead); writing—review and editing (lead). **Younggap Lim:** Conceptualization (supporting); data curation (equal); formal analysis (supporting); investigation (equal); methodology (supporting); validation (supporting); visualization (supporting); writing—original draft (supporting); writing—review and editing (supporting). **Ji Sun Jang:** Data curation (supporting); investigation (supporting); methodology (supporting); resources (equal); validation (supporting); writing—original draft (supporting); writing—review and editing (supporting). **Yeon Kyeong Ko:** Data curation (supporting); investigation (supporting); validation (supporting); visualization (supporting); writing—original draft (supporting); writing—review and editing (supporting). **Youngnim Choi:** Conceptualization (supporting); data curation (supporting); investigation (supporting); methodology (supporting); supervision (supporting); writing—review and editing (supporting). **Hong-Hee Kim:** Project administration (supporting); resources (supporting); supervision (supporting); writing—review and editing (supporting). **Bong-Kyu Choi:** Conceptualization (lead); data curation (equal); funding acquisition (supporting); project administration (lead); resources (lead); supervision (lead); writing—original draft (lead); writing—review and editing (lead).

## ACKNOWLEDGEMENTS

This work was supported by grants from the National Research Foundation of Korea (NRF-2022R1C1C2007752) and the Dental Research Institute of Seoul National University.

## CONFLICT OF INTEREST STATEMENT

The authors declare no competing interests.

## DATA AVAILABILITY STATEMENT

The data that support the findings of this study are available from the corresponding author upon reasonable request.

## ORCID

Bong-Kyu Choi  <https://orcid.org/0000-0003-3743-7209>

## REFERENCES

- Acharya, C., Sahingur, S. E., & Bajaj, J. S. (2017). Microbiota, cirrhosis, and the emerging oral-gut-liver axis. *JCI Insight*, 2(19), e94416.
- Ahn, J., Han, K. S., Heo, J. H., Bang, D., Kang, Y. H., Jin, H. A., Hong, S. J., Lee, J. H., & Ham, W. S. (2016). FOXC2 and CLIP4: A potential biomarker for synchronous metastasis of  $\leq 7$ -cm clear cell renal cell carcinomas. *Oncotarget*, 7(32), 51423–51434.
- Akinkugbe, A. A., Avery, C. L., Barritt, A. S., Cole, S. R., Lerch, M., Mayerle, J., Offenbacher, S., Petersmann, A., Nauck, M., Volzke, H., Slade, G. D., Heiss, G., Kocher, T., & Holtfreter, B. (2017). Do genetic markers of inflammation modify the relationship between periodontitis and nonalcoholic fatty liver disease? Findings from the SHIP study. *Journal of Dental Research*, 96(12), 1392–1399.
- Alessi, M. C., Bastelica, D., Mavri, A., Morange, P., Berthet, B., Grino, M., & Juhan-Vague, I. (2003). Plasma PAI-1 levels are more strongly related to liver steatosis than to adipose tissue accumulation. *Arteriosclerosis Thrombosis and Vascular Biology*, 23(7), 1262–1268.
- Alessi, M. C., & Juhan-Vague, I. (2006). PAI-1 and the metabolic syndrome—Links, causes, and consequences. *Arteriosclerosis Thrombosis and Vascular Biology*, 26(10), 2200–2207.
- Alessi, M. C., Peiretti, F., Morange, P., Henry, M., Nalbone, G., & Juhan-Vague, I. (1997). Production of plasminogen activator inhibitor 1 by human adipose tissue—Possible link between visceral fat accumulation and vascular disease. *Diabetes*, 46(5), 860–867.
- Alsharoh, H., Ismaiel, A., Leucuta, D. C., Popa, S. L., & Dumitrascu, D. L. (2022). Plasminogen activator inhibitor-1 levels in non-alcoholic fatty liver disease: A systematic review and meta-analysis. *Journal of Gastrointestinal and Liver Diseases*, 31(2), 206–214.
- Aron-Wisniewsky, J., Vigliotti, C., Witjes, J., Le, P., Holleboom, A. G., Verheij, J., Nieuwdorp, M., & Clement, K. (2020). Gut microbiota and human NAFLD: Disentangling microbial signatures from metabolic disorders. *Nature Reviews Gastroenterology & Hepatology*, 17(5), 279–297.
- Bizzarro, S., van der Velden, U., ten Heggeler, J. M. A. G., Leivadarios, E., Hoek, F. J., Gerdes, V. E. A., Bakker, S. J. L., Gans, R. O. B., ten Cate, H., & Loos, B. G. (2007). Periodontitis is characterized by elevated PAI-1 activity. *Journal of Clinical Periodontology*, 34(7), 574–580.
- Busso, N., Nicodeme, E., Chesne, C., Guillouzo, A., Belin, D., & Hyafil, F. (1994). Urokinase and type I plasminogen activator inhibitor production by normal human hepatocytes: Modulation by inflammatory agents. *Hepatology*, 20(1 Pt 1), 186–190.
- Cani, P. D., Amar, J., Iglesias, M. A., Poggi, M., Knauf, C., Bastelica, D., Neyrinck, A. M., Fava, F., Tuohy, K. M., Chabo, C., Waget, A., Delmee, E., Cousin, B., Sulpice, T., Chamontin, B., Ferrieres, J., Tanti, J. F., Gibson, G. R., Casteilla, L., ... Burcelin, R. (2007). Metabolic endotoxemia initiates obesity and insulin resistance. *Diabetes*, 56(7), 1761–1772.
- Carpino, G., Del Ben, M., Pastori, D., Carnevale, R., Baratta, F., Overi, D., Francis, H., Cardinale, V., Onori, P., Safarikia, S., Cammisotto, V., Alvaro, D., Svegliati-Baroni, G., Angelico, F., Gaudio, E., & Violi, F. (2020). Increased liver localization of lipopolysaccharides in human and experimental NAFLD. *Hepatology*, 72(2), 470–485.
- Chalasanani, N., Younossi, Z., Lavine, J. E., Diehl, A. M., Brunt, E. M., Cusi, K., Charlton, M., Sanyal, A. J., American Gastroenterological, A., American Association for the Study of Liver, D., & American College of, G. (2012). The diagnosis and management of non-alcoholic fatty liver disease: Practice guideline by the

- American Gastroenterological Association, American Association for the Study of Liver Diseases, and American College of Gastroenterology. *Gastroenterology*, 142(7), 1592–1609.
- Chen, T.-P., Yu, H.-C., Lin, W.-Y., & Chang, Y.-C. (2023). The role of microbiome in the pathogenesis of oral-gut-liver axis between periodontitis and nonalcoholic fatty liver disease. *Journal of Dental Sciences*, 18(3), 972–975.
- Dimova, E., & Kietzmann, T. (2008). Metabolic, hormonal and environmental regulation of plasminogen activator inhibitor-1 (PAI-1) expression: Lessons from the liver. *Thrombosis and Haemostasis*, 100(6), 992–1006.
- Duarte, S. M. B., Stefano, J. T., Miele, L., Ponziani, F. R., Souza-Basqueira, M., Okada, L. S. R. R., Costa, F. G. D., Toda, A. K., Mazo, D. F. C., Sabino, E. C., Carrilho, E. J., Gasbarrini, A., & Oliveira, C. P. (2018). Gut microbiome composition in lean patients with NASH is associated with liver damage independent of caloric intake: A prospective pilot study. *Nutrition Metabolism and Cardiovascular Diseases*, 28(4), 369–384.
- Ekstedt, M., Nasr, P., & Kechagias, S. (2017). Natural history of NAFLD/NASH. *Current Hepatology Reports*, 16(4), 391–397.
- Erickson, L. A., Schleaf, R. R., Ny, T., & Loskutoff, D. J. (1985). The fibrinolytic system of the vascular wall. *Clinics in Haematology*, 14(2), 513–530.
- Fizanne, L., Villard, A., Benabbou, N., Recoquillon, S., Soleti, R., Delage, E., Wertheimer, M., Vidal-Gomez, X., Oullier, T., Chaffron, S., Martinez, M. C., Neunlist, M., Boursier, J., & Andriantsitohaina, R. (2023). Faeces-derived extracellular vesicles participate in the onset of barrier dysfunction leading to liver diseases. *Journal of Extracellular Vesicles*, 12(2), e12303.
- Fuhrmeister, J., Zota, A., Sijmonsma, T. P., Seibert, O., Cingir, S., Schmidt, K., Vallon, N., de Guia, R. M., Niopek, K., Berriel Diaz, M., Maida, A., Bluher, M., Okun, J. G., Herzig, S., & Rose, A. J. (2016). Fasting-induced liver GADD45 $\beta$  restrains hepatic fatty acid uptake and improves metabolic health. *EMBO Molecular Medicine*, 8(6), 654–669.
- Fujita, M., Kuraji, Y., Ito, H., Hashimoto, S., Toen, T., Fukada, T., & Numabe, Y. (2018). Histological effects and pharmacokinetics of lipopolysaccharide derived from *Porphyromonas gingivalis* on rat maxilla and liver concerning with progression into non-alcoholic steatohepatitis. *Journal of Periodontology*, 89(9), 1101–1111.
- Genco, R. J., & Borgnakke, W. S. (2013). Risk factors for periodontal disease. *Periodontology 2000*, 62(1), 59–94.
- Gu, Z. L., Li, F. Y., Liu, Y. H., Jiang, M. W., Zhang, L. H., He, L. Q., Wilkey, D. W., Merchant, M., Zhang, X., Deng, Z. B., Chen, S. Y., Barve, S., McClain, C. J., & Feng, W. K. (2021). Exosome-like nanoparticles from *Lactobacillus rhamnosus* GG protect against alcohol-associated liver disease through intestinal aryl hydrocarbon receptor in mice. *Hepatology Communications*, 5(5), 846–864.
- Han, E. C., Choi, S. Y., Lee, Y., Park, J. W., Hong, S. H., & Lee, H. J. (2019). Extracellular RNAs in periodontopathogenic outer membrane vesicles promote TNF- $\alpha$  production in human macrophages and cross the blood-brain barrier in mice. *FASEB Journal*, 33(12), 13412–13422.
- Han, P. P., Bartold, P. M., Salomon, C., & Ivanovski, S. (2021). Salivary outer membrane vesicles and DNA methylation of small extracellular vesicles as biomarkers for periodontal status: A pilot study. *International Journal of Molecular Sciences*, 22(5), 2423.
- Hashimoto, M., Tawaratsumida, K., Kariya, H., Aoyama, K., Tamura, T., & Suda, Y. (2006). Lipoprotein is a predominant Toll-like receptor 2 ligand in *Staphylococcus aureus* cell wall components. *International Immunology*, 18(2), 355–362.
- Helenius-Hietala, J., Suominen, A. L., Ruokonen, H., Knuutila, M., Puukka, P., Jula, A., Meurman, J. H., & Aberg, F. (2019). Periodontitis is associated with incident chronic liver disease—A population-based cohort study. *Liver International*, 39(3), 583–591.
- Henaoui-Mejia, J., Elinav, E., Jin, C. C., Hao, L. M., Mehal, W. Z., Strowig, T., Thaiss, C. A., Kau, A. L., Eisenbarth, S. C., Jurczak, M. J., Camporez, J. P., Shulman, G. I., Gordon, J. I., Hoffman, H. M., & Flavell, R. A. (2012). Inflammation-mediated dysbiosis regulates progression of NAFLD and obesity. *Nature*, 482(7384), 179–185.
- Henkel, A. S., Khan, S. S., Olivares, S., Miyata, T., & Vaughan, D. E. (2018). Inhibition of plasminogen activator inhibitor 1 attenuates hepatic steatosis but does not prevent progressive nonalcoholic steatohepatitis in mice. *Hepatology Communications*, 2(12), 1479–1492.
- Himes, R. W., & Smith, C. W. (2010). Tlr2 is critical for diet-induced metabolic syndrome in a murine model. *FASEB Journal*, 24(3), 731–739.
- Hong, G. P., Kim, M. H., & Kim, H. J. (2021). Sex-related differences in glial fibrillary acidic protein-positive GABA regulate neuropathology following pilocarpine-induced status epilepticus. *Neuroscience*, 472, 157–166.
- Imajo, K., Fujita, K., Yoneda, M., Nozaki, Y., Ogawa, Y., Shinohara, Y., Kato, S., Mawatari, H., Shibata, W., Kitani, H., Ikejima, K., Kirikoshi, H., Nakajima, N., Saito, S., Maeyama, S., Watanabe, S., Wada, K., & Nakajima, A. (2012). Hyperresponsivity to low-dose endotoxin during progression to nonalcoholic steatohepatitis is regulated by leptin-mediated signaling. *Cell Metabolism*, 16(1), 44–54.
- Jang, S. C., Kim, S. R., Yoon, Y. J., Park, K. S., Kim, J. H., Lee, J., Kim, O. Y., Choi, E. J., Kim, D. K., Choi, D. S., Kim, Y. K., Park, J., Di Vizio, D., & Gho, Y. S. (2015). In vivo kinetic biodistribution of nano-sized outer membrane vesicles derived from bacteria. *Small*, 11(4), 456–461.
- Jun, H. K., Jung, Y. J., Ji, S., An, S. J., & Choi, B. K. (2018). Caspase-4 activation by a bacterial surface protein is mediated by cathepsin G in human gingival fibroblasts. *Cell Death and Differentiation*, 25(2), 380–391.
- Jung, Y. J., Jun, H. K., & Choi, B. K. (2017). *Porphyromonas gingivalis* suppresses invasion of *Fusobacterium nucleatum* into gingival epithelial cells. *Journal of Oral Microbiology*, 9(1), 1320193.
- Kanuri, G., Spruss, A., Wagnerberger, S., Bischoff, S. C., & Bergheim, I. (2011). Fructose-induced steatosis in mice: Role of plasminogen activator inhibitor-1, microsomal triglyceride transfer protein and NKT cells. *Laboratory Investigation*, 91(6), 885–895.
- Kim, H. Y., Lim, Y., An, S. J., & Choi, B. K. (2020). Characterization and immunostimulatory activity of extracellular vesicles from *Filifactor alocis*. *Molecular Oral Microbiology*, 35(1), 1–9.
- Kim, H. Y., Song, M. K., Gho, Y. S., Kim, H. H., & Choi, B. K. (2021). Extracellular vesicles derived from the periodontal pathogen *Filifactor alocis* induce systemic bone loss through Toll-like receptor 2. *Journal of Extracellular Vesicles*, 10(12), e12157.
- Kim, H. Y., Song, M. K., Lim, Y., Jang, J. S., An, S. J., Kim, H. H., & Choi, B. K. (2022). Effects of extracellular vesicles derived from oral bacteria on osteoclast differentiation and activation. *Scientific Reports*, 12(1), 14239.
- Kinane, D. F., Stathopoulou, P. G., & Papananou, P. N. (2017). Periodontal diseases. *Nature Reviews Disease Primers*, 3, 17038.
- Klarstrom Engstrom, K., Khalaf, H., Kalvegren, H., & Bengtsson, T. (2015). The role of *Porphyromonas gingivalis* gingipains in platelet activation and innate immune modulation. *Molecular Oral Microbiology*, 30(1), 62–73.
- Komazaki, R., Katagiri, S., Takahashi, H., Maekawa, S., Shiba, T., Takeuchi, Y., Kitajima, Y., Ohtsu, A., Udagawa, S., Sasaki, N., Watanabe, K., Sato, N., Miyasaka, N., Eguchi, Y., Anzai, K., & Izumi, Y. (2017). Periodontal pathogenic bacteria, *Aggregatibacter actinomycetemcomitans* affect non-alcoholic fatty liver disease by altering gut microbiota and glucose metabolism. *Scientific Reports*, 7, 13950.
- Kono, H., Uesugi, T., Froh, M., Rusyn, I., Bradford, B. U., & Thurman, R. G. (2001). ICAM-1 is involved in the mechanism of alcohol-induced liver injury: Studies with knockout mice. *American Journal of Physiology-Gastrointestinal and Liver Physiology*, 280(6), G1289–G1295.
- Kumar, A., Sundaram, K., Mu, J., Dryden, G. W., Sriwastava, M. K., Lei, C., Zhang, L., Qiu, X., Xu, F., Yan, J., Zhang, X., Park, J. W., Merchant, M. L., Bohler, H. C. L., Wang, B., Zhang, S., Qin, C., Xu, Z., Han, X., ... Zhang, H. G. (2021). High-fat diet-induced upregulation of exosomal phosphatidylcholine contributes to insulin resistance. *Nature Communications*, 12(1), 213.



- Lee, C. C., Avalos, A. M., & Ploegh, H. L. (2012). Accessory molecules for Toll-like receptors and their function. *Nature Reviews Immunology*, 12(3), 168–179.
- Lee, G., You, H. J., Bajaj, J. S., Joo, S. K., Yu, J., Park, S., Kang, H., Park, J. H., Kim, J. H., Lee, D. H., Lee, S., Kim, W., & Ko, G. (2020). Distinct signatures of gut microbiome and metabolites associated with significant fibrosis in non-obese NAFLD. *Nature Communications*, 11(1), 4982.
- Lee, S. M., Dorotea, D., Jung, I., Nakabayashi, T., Miyata, T., & Ha, H. (2017). TM5441, a plasminogen activator inhibitor-1 inhibitor, protects against high fat diet-induced non-alcoholic fatty liver disease. *Oncotarget*, 8(52), 89746–89760.
- Levine, J. A., Oleaga, C., Eren, M., Amaral, A. P., Shang, M., Lux, E., Khan, S. S., Shah, S. J., Omura, Y., Pamir, N., Hay, J., Barish, G., Miyata, T., Tavori, H., Fazio, S., & Vaughan, D. E. (2021). Role of PAI-1 in hepatic steatosis and dyslipidemia. *Scientific Reports*, 11(1), 430.
- Lopez-Aleman, R., Redondo, J. M., Nagamine, Y., & Munoz-Canoves, P. (2003). Plasminogen activator inhibitor type-1 inhibits insulin signaling by competing with  $\alpha\beta 3$  integrin for vitronectin binding. *European Journal of Biochemistry*, 270(5), 814–821.
- Luther, J., Garber, J. J., Khalili, H., Dave, M., Bale, S. S., Jindal, R., Motola, D. L., Luther, S., Bohr, S., Jeoung, S. W., Deshpande, V., Singh, G., Turner, J. R., Yarmush, M. L., Chung, R. T., & Patel, S. J. (2015). Hepatic injury in nonalcoholic steatohepatitis contributes to altered intestinal permeability. *Cellular and Molecular Gastroenterology and Hepatology*, 1(2), 222–232.
- MacParland, S. A., Liu, J. C., Ma, X. Z., Innes, B. T., Bartczak, A. M., Gage, B. K., Manuel, J., Khuu, N., Echeverri, J., Linares, I., Gupta, R., Cheng, M. L., Liu, L. Y., Camat, D., Chung, S. W., Seliga, R. K., Shao, Z. G., Lee, E., Ogawa, S., ... McGilvray, I. D. (2018). Single cell RNA sequencing of human liver reveals distinct intrahepatic macrophage populations. *Nature Communications*, 9, 4383.
- Miura, K., & Ohnishi, H. (2014). Role of gut microbiota and toll-like receptors in nonalcoholic fatty liver disease. *World Journal of Gastroenterology*, 20(23), 7381–7391.
- Miura, K., Ohnishi, H., & Seki, E. (2012). Palmitic acid and TLR2 cooperatively contribute to the development of nonalcoholic steatohepatitis through inflammasome activation. *Gastroenterology*, 142(5), S920–S921.
- Naldini, L., Vigna, E., Bardelli, A., Follenzi, A., Galimi, F., & Comoglio, P. M. (1995). Biological activation of pro-HGF (hepatocyte growth-factor) by urokinase is controlled by a stoichiometric reaction. *Journal of Biological Chemistry*, 270(2), 603–611.
- Raftar, S. K. A., Ashrafian, F., Abdollahiyan, S., Yadegar, A., Moradi, H. R., Masoumi, M., Vaziri, F., Moshiri, A., Siadat, S. D., & Zali, M. R. (2022). The anti-inflammatory effects of *Akkermansia muciniphila* and its derivatives in HFD/CCL4-induced murine model of liver injury. *Scientific Reports*, 12(1), 2453.
- Rivas, G., Hummer-Bair, B., Bezinover, D., Kadry, Z., & Stine, J. (2021). Plasminogen activator inhibitor is significantly elevated in liver transplant recipients with decompensated NASH cirrhosis. *BMJ Open Gastroenterology*, 8(1), e000683.
- Roth, G. A., Moser, B., Huang, S. J., Brandt, J. S., Huang, Y., Papapanou, P. N., Schmidt, A. M., & Lalla, E. (2006). Infection with a periodontal pathogen induces procoagulant effects in human aortic endothelial cells. *Journal of Thrombosis and Haemostasis*, 4(10), 2256–2261.
- Sasaki, N., Katagiri, S., Komazaki, R., Watanabe, K., Maekawa, S., Shiba, T., Udagawa, S., Takeuchi, Y., Ohtsu, A., Kohda, T., Tohara, H., Miyasaka, N., Hirota, T., Tamari, M., & Izumi, Y. (2018). Endotoxemia by *Porphyromonas gingivalis* injection aggravates non-alcoholic fatty liver disease, disrupts glucose/lipid metabolism, and alters gut microbiota in mice. *Frontiers in Microbiology*, 9, 2470.
- Sato, S., Kamata, Y., Kessoku, T., Shimizu, T., Kobayashi, T., Kurihashi, T., Takashiba, S., Hatanaka, K., Hamada, N., Kodama, T., Higurashi, T., Taguri, M., Yoneda, M., Usuda, H., Wada, K., Nakajima, A., Morozumi, T., & Minabe, M. (2022). A cross-sectional study assessing the relationship between non-alcoholic fatty liver disease and periodontal disease. *Scientific Reports*, 12(1), 13621.
- Sayin, S. I., Wahlstrom, A., Felin, J., Jantti, S., Marschall, H. U., Bamberg, K., Angelin, B., Hyotylainen, T., Oresic, M., & Backhed, F. (2013). Gut microbiota regulates bile acid metabolism by reducing the levels of tauro-beta-muricholic acid, a naturally occurring FXR antagonist. *Cell metabolism*, 17(2), 225–235.
- Sender, R., Fuchs, S., & Milo, R. (2016). Revised estimates for the number of human and bacterial cells in the body. *PLoS Biology*, 14(8), e1002533.
- Seo, H. S., & Nahm, M. H. (2009). Lipoprotein lipase and hydrofluoric acid deactivate both bacterial lipoproteins and lipoteichoic acids, but platelet-activating factor-acetylhydrolase degrades only lipoteichoic acids. *Clinical and Vaccine Immunology*, 16(8), 1187–1195.
- Seyama, M., Yoshida, K., Yoshida, K., Fujiwara, N., Ono, K., Eguchi, T., Kawai, H., Guo, J. J., Weng, Y., Haoze, Y., Uchibe, K., Ikegame, M., Sasaki, A., Nagatsuka, H., Okamoto, K., Okamura, H., & Ozaki, K. (2020). Outer membrane vesicles of *Porphyromonas gingivalis* attenuate insulin sensitivity by delivering gingipains to the liver. *Biochimica et Biophysica Acta-Molecular Basis of Disease*, 1866(6), 165731.
- Song, L. T., Tada, H., Nishioka, T., Nemoto, E., Imamura, T., Potempa, J., Li, C. Y., Matsushita, K., & Sugawara, S. (2021). *Porphyromonas gingivalis* gingipain-mediated degradation of plasminogen activator inhibitor-1 leads to delayed wound healing responses in human endothelial cells. *Journal of Innate Immunity*, 14(4), 306–319.
- Song, M. K., Kim, H. Y., Choi, B. K., & Kim, H. H. (2020). *Filifactor alocis*-derived extracellular vesicles inhibit osteogenesis through TLR2 signaling. *Molecular Oral Microbiology*, 35(5), 202–210.
- Suppli, M. P., Bagger, J. I., Lelouvier, B., Broha, A., Demant, M., Konig, M. J., Strandberg, C., Lund, A., Vilsboll, T., & Knop, F. K. (2021). Hepatic microbiome in healthy lean and obese humans. *JHEP Reports*, 3(4), 100299.
- Targher, G., Marra, F., & Marchesini, G. (2008). Increased risk of cardiovascular disease in non-alcoholic fatty liver disease: Causal effect or epiphenomenon? *Diabetologia*, 51(11), 1947–1953.
- Toyofuku, M., Nomura, N., & Eberl, L. (2019). Types and origins of bacterial membrane vesicles. *Nature Reviews Microbiology*, 17(1), 13–24.
- Utzschneider, K. M., & Kahn, S. E. (2006). Review: The role of insulin resistance in nonalcoholic fatty liver disease. *The Journal of Clinical Endocrinology & Metabolism*, 91(12), 4753–4761.
- Veith, P. D., Chen, Y. Y., Gorasia, D. G., Chen, D., Glew, M. D., O'Brien-Simpson, N. M., Cecil, J. D., Holden, J. A., & Reynolds, E. C. (2014). *Porphyromonas gingivalis* outer membrane vesicles exclusively contain outer membrane and periplasmic proteins and carry a cargo enriched with virulence factors. *Journal of Proteome Research*, 13(5), 2420–2432.
- Wang, T., Ishikawa, T., Sasaki, M., & Chiba, T. (2022). Oral and gut microbial dysbiosis and non-alcoholic fatty liver disease: The central role of *Porphyromonas gingivalis*. *Frontiers in Medicine*, 9, 822190.
- Xu, Y. Y., Wu, Y. H., Xiong, Y., Tao, J. W., Pan, T. C., Tan, S. L., Gao, G., Chen, Y., Abbas, N., Getachew, A., Zhuang, Y. Q., You, K., Yang, F., & Li, Y. X. (2020). Ascorbate protects liver from metabolic disorder through inhibition of lipogenesis and suppressor of cytokine signaling 3 (SOCS3). *Nutrition & Metabolism*, 17(1), 17.
- Yang, L., Li, P., Fu, S., Calay, E. S., & Hotamisligil, G. S. (2010). Defective hepatic autophagy in obesity promotes ER stress and causes insulin resistance. *Cell Metabolism*, 11(6), 467–478.
- Ye, Q., Zou, B. Y., Yeo, Y. H., Li, J., Huang, D. Q., Wu, Y. K., Yang, H. L., Liu, C. L., Kam, L. Y., Tan, X. X. E., Chien, N., Trinh, S., Henry, L., Stave, C. D., Hosaka, T., Cheung, R. C., & Nguyen, M. H. (2020). Global prevalence, incidence, and outcomes of non-obese or lean non-alcoholic fatty liver disease: A systematic review and meta-analysis. *Lancet Gastroenterology & Hepatology*, 5(8), 739–752.

- Yoneda, M., Naka, S., Nakano, K., Wada, K., Endo, H., Mawatari, H., Imajo, K., Nomura, R., Hokamura, K., Ono, M., Murata, S., Tohnai, I., Sumida, Y., Shima, T., Kuboniwa, M., Umemura, K., Kamisaki, Y., Amano, A., Okanoue, T., ... Nakajima, A. (2012). Involvement of a periodontal pathogen, *Porphyromonas gingivalis* on the pathogenesis of non-alcoholic fatty liver disease. *BMC Gastroenterology*, *12*, 16.
- Yu, Y., Cai, J., She, Z., & Li, H. (2019). Insights into the epidemiology, pathogenesis, and therapeutics of nonalcoholic fatty liver diseases. *Advanced Science (Weinh)*, *6*(4), 1801585.
- Zahmatkesh, M. E., Jahanbakhsh, M., Hoseini, N., Shegefti, S., Peymani, A., Dabin, H., Samimi, R., & Bolori, S. (2022). Effects of exosomes derived from *Helicobacter pylori* outer membrane vesicle-infected hepatocytes on hepatic stellate cell activation and liver fibrosis induction. *Frontiers in Cellular and Infection Microbiology*, *12*, 857570.
- Zhu, L., Baker, S. S., Gill, C., Liu, W., Alkhoury, R., Baker, R. D., & Gill, S. R. (2013). Characterization of gut microbiomes in nonalcoholic steatohepatitis (NASH) patients: A connection between endogenous alcohol and NASH. *Hepatology*, *57*(2), 601–609.

## SUPPORTING INFORMATION

Additional supporting information can be found online in the Supporting Information section at the end of this article.

**How to cite this article:** Kim, H. Y., Lim, Y., Jang, J. S., Ko, Y. K., Choi, Y., Kim, H.-H., & Choi, B.-K. (2024). Extracellular vesicles from periodontal pathogens regulate hepatic steatosis via Toll-like receptor 2 and plasminogen activator inhibitor-1. *Journal of Extracellular Vesicles*, *13*, e12407. <https://doi.org/10.1002/jev2.12407>